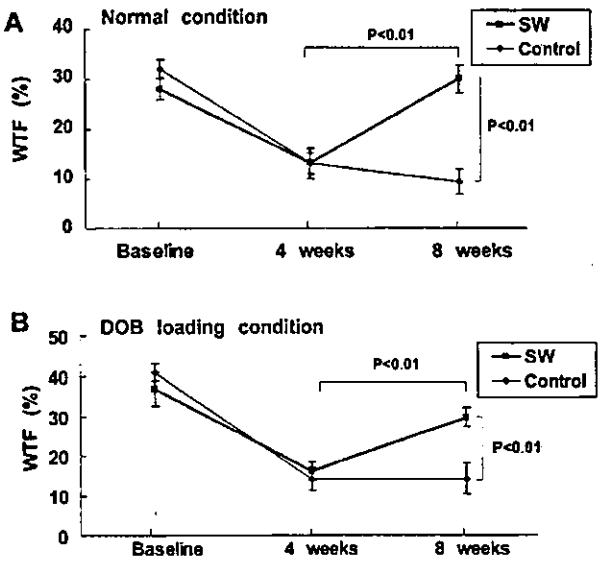

Figure 5. Extracorporeal cardiac SW therapy improves regional myocardial function in vivo. SW therapy induced a complete recovery of WTF of the ischemic lateral wall under control conditions (A) and under dobutamine (DOB) loading conditions (B). Results are expressed as mean±SEM (n=8 each).

control group and 1.4±0.3 in the SW group, $P<0.05$; Figure 6A) as well as in the epicardium (0.7±0.2 in the control group and 1.5±0.2 in the SW group, $P<0.05$; Figure 6B).

Effects of Extracorporeal Cardiac SW Therapy on Capillary Density and VEGF Expression in the Ischemic Myocardium

Factor VIII staining showed that the number of factor VIII–positive capillaries was increased in the SW group compared with the control group (Figure 7A and 7B). Quantitative analysis demonstrated that the number of capillaries was significantly higher in the SW group in both the endocardium (840±26 in the control group and 1280±45 in the SW group, $P<0.05$; Figure 7C) and the epicardium (820±30 in the control group and 1200±22 in the SW group, $P<0.05$; Figure 7D). RT-PCR analysis and Western blotting demonstrated a significant upregulation of VEGF mRNA expression (8.0±6 in the control group and 32±8 in the SW group, $P<0.05$; Figure 8A) and protein expression (2.23-fold increase in the SW groups, $P<0.05$; Figure 8B) after the SW treatment to the ischemic myocardium in vivo.

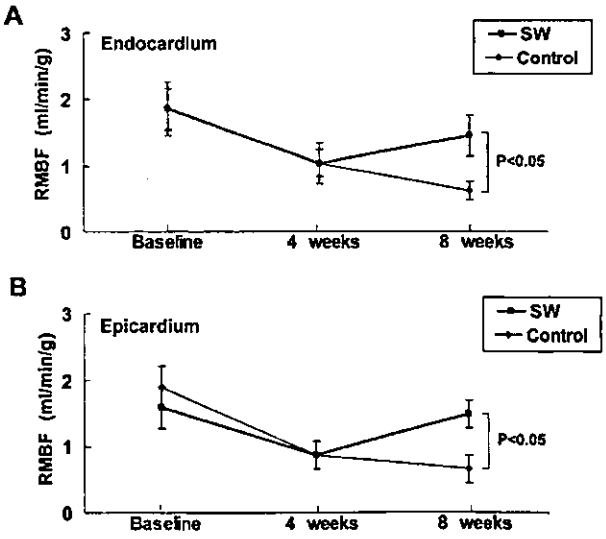

Figure 6. Extracorporeal cardiac SW therapy improves RMBF in vivo. SW therapy significantly increased RMBF, assessed by colored microspheres in both the endocardium (A) and the epicardium (B). Results are expressed as mean±SEM (n=8 each).

Side Effects of Extracorporeal Cardiac SW Therapy

All animals treated with the SW therapy were alive and showed no arrhythmias as assessed by 24-hour Holter ECG during and after the treatment (n=3; data not shown). There also was no myocardial cell damage as assessed by serum concentrations of CK-MB (ng/mL); the values before the SW treatment and at 4, 5 (2 hours after the SW treatment), and 8 weeks after the ameroid implantation were 5.0±0.6, 6.2±0.5, 5.5±0.2, and 7.1±0.9 in the control group and 5.1±0.2, 7.7±0.6, 6.1±0.6, and 6.4±0.4 in the SW group, respectively (n=6 each). The serum concentrations of troponin T were not detected in most cases in both groups. No significant differences were noted in hemodynamic variables (eg, heart rate or blood pressure) between the 2 groups (data not shown).

Discussion

The novel finding of the present study is that the extracorporeal cardiac SW therapy enhances angiogenesis in the ischemic myocardium and normalizes myocardial function in a porcine model of chronic myocardial ischemia in vivo. To the best of our knowledge, this is the first report that demonstrates the potential usefulness of extracorporeal cardiac SW therapy as a noninvasive treatment of chronic myocardial ischemia.

Extracorporeal Cardiac SW Therapy as a Novel Strategy for Ischemic Cardiomyopathy

Because of the poor prognosis of ischemic cardiomyopathy,[1,9] it is crucial to develop an alternative therapy for ischemia-induced myocardial dysfunction. To accomplish effective angiogenesis, it is mandatory to upregulate potent angiogenesis ligands, such as VEGF, and their receptors.[9,10] Furthermore, in the clinical setting, the goal for the treatment of ischemic cardiomyopathy should include not only enhancement of angiogenesis but also recovery of ischemia-induced myocardial dysfunction. In the present study, we were able to demonstrate that SW treatment (1) normalized global and regional myocardial functions as well as RMBF of the chronic ischemic region without any adverse effects in vivo, (2) increased vascular density in the SW-treated region, and (3) enhanced mRNA expression of VEGF and its receptor Flt-1 in HUVECs in vitro and VEGF production in the ischemic myocardium in vivo. Thus, SW-induced upregulation of the endogenous angiogenic system may offer a novel and promising noninvasive strategy for the treatment of ischemic heart disease.

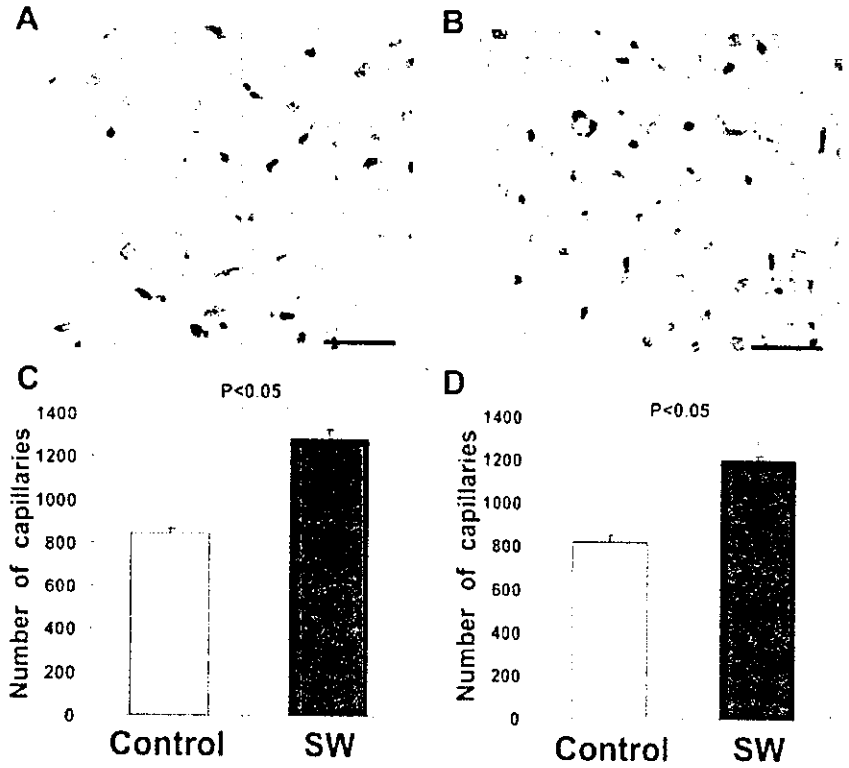

Figure 7. Extracorporeal cardiac SW therapy increases the density of factor VIII–positive capillaries in the ischemic myocardium. A and B, Factor VIII staining of the LCx region from the control (A) and the SW group (B). Scale bar represents 20 μm. C and D, Capillary density was significantly greater in the SW group (SW) than in the control group (Control) in both the endocardium (C) and the epicardium (D). Results are expressed as mean±SEM (n=6 each).

Advantages of Extracorporeal Cardiac SW Therapy

Recent attempts to enhance angiogenesis in the ischemic organs include gene therapy and bone marrow cell transplantation therapy. The main purpose of gene therapy is to induce overexpression of a selected angiogenic ligand (eg, VEGF) that leads to angiogenesis in the ischemic region. Although phase I trials of gene transfer of plasmid DNA encoding VEGF demonstrated safety and clinical benefit for the treatment of ischemic limb and heart,[11–13] gene therapy for ischemic cardiomyopathy is still at a preclinical stage. Bone marrow cell transplantation therapy, which depends on adult stem cell plasticity, also may be a useful strategy for angiogenesis because endothelial progenitor cells could be isolated from circulating mononuclear cells in humans and could be shown to be incorporated into neovascularization.[14] However, the need for invasive delivery of those cells to the ischemic myocardium may severely limit its usefulness in clinical situations.

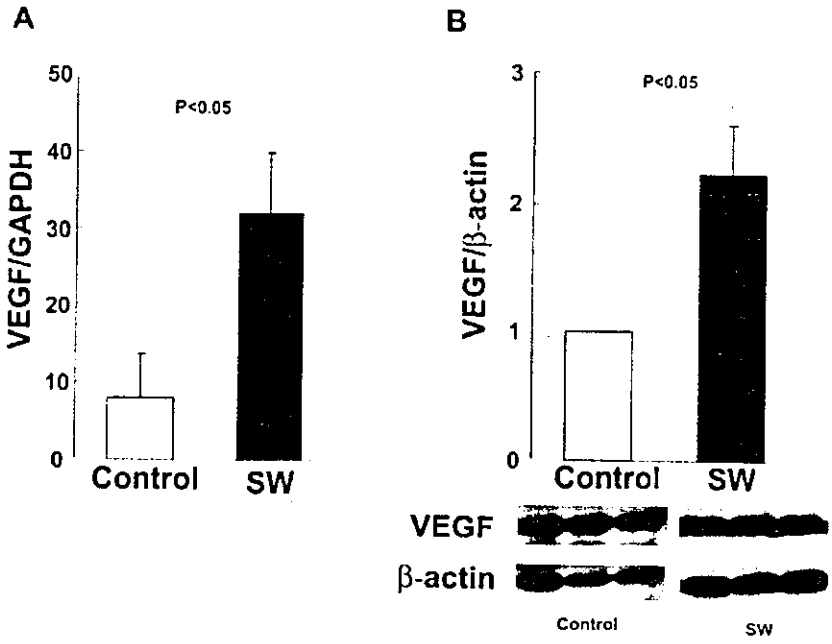

Figure 8. SW treatment upreglated mRNA (A) and protein (B) expression of VEGF in the ischemic myocardium (n=5 each).

A major advantage of the extracorporeal cardiac SW therapy over these 2 strategies is shown by the fact that it is quite noninvasive and safe, without any adverse effects. If necessary, we could repeatedly treat patients (even outpatients) with SW therapy because no surgery, anesthesia, or even catheter intervention is required for the treatment. This is an important factor in determining the clinical usefulness of angiogenic therapies in patients with ischemic cardiomyopathy. Thus, the extracorporeal cardiac SW therapy appears to be an applicable and noninvasive treatment for ischemic heart disease. Indeed, the SW treatment itself already has been clinically established as an effective and safe treatment for lithotripsy and chronic plantar fasciitis.[15,16] Our present results indicate that SW therapy, at ≈10% of the energy needed for lithotripsy treatment, is effective for in vivo angiogenesis in the ischemic heart.

Mechanisms for SW-Induced Angiogenesis

When a SW hits tissue, cavitation (a micrometer-sized violent collapse of bubbles) is induced by the first compression by the positive pressure part and the expansion with the tensile part of a SW.[3] Because the physical forces generated by cavitation are highly localized, SW could induce localized stress on cell membranes, as altered shear stress affects endothelial cells.[17] Recent reports have demonstrated the biochemical effects of SW, including hyperpolarization and Ras activation,[18] nonenzymatic nitric oxide synthesis,[19] and induction of stress fibers and intercellular gaps.[20] Although precise mechanisms for the SW-induced biochemical effects remain to be examined, these mechanisms may be involved in the underlying mechanisms for SW-induced angiogenesis. Indeed, Wang et al[21] reported that SW induces angiogenesis of the Achilles tendon–bone junction in dogs.

We were able to demonstrate that the SW treatment upregulated mRNA expression of VEGF and its receptor Flt in HUVECs in vitro and VEGF expression in the ischemic myocardium in vivo. Because the VEGF-Flt system is essential in initiating vasculogenesis and/or angiogenesis,[22] this effect of SW could explain, at least in part, the underlying mechanisms for SW-induced angiogenesis. It should be noted, however, that we showed only the upregulation of VEGF and Flt and that the effect of SW on signal transduction after receptor–ligand interaction still remains to be clarified. In addition, we need to fully elucidate the mechanisms for the SW-induced complete recovery of ischemia-induced myocardial dysfunction, although the increased myocardial blood flow caused by the SW treatment appears to play a primary role for the improved myocardial function. Further studies are required to determine the precise molecular mechanism for SW-induced angiogenesis and recovery of myocardial function.

In summary, we were able to demonstrate that noninvasive extracorporeal cardiac SW therapy effectively increases RMBF and normalizes ischemia-induced myocardial dysfunction without any adverse effects. Thus, extracorporeal cardiac SW therapy may be an effective, safe, and noninvasive therapy for ischemic cardiomyopathy.

Acknowledgments

This study was supported in part by a grant from the 21st Century COE Program and grants-in-aid from the Japanese Ministry of Education, Culture, Sports, Science, and Technology, Tokyo, Japan (Nos. 12032215, 12470158, 12877114, 13307024, 13557068), and the Japanese Ministry of Health, Labor, and Welfare, Tokyo, Japan. We thank Dr Ernest H. Marlinghaus, Storz Medical AG, Switzerland, for valuable discussion about our study, and Prof S. Mohri at the Center of Biomedical Research, Kyushu University Graduate School of Medical Sciences, for cooperation in this study.

References

1. Jessup M, Brozena S. Heart failure. *N Engl J Med*. 2003;348:2007–2018.
2. Gutersohn A, Caspari G. Shock waves upregulate vascular endothelial growth factor m-RNA in human umbilical vascular endothelial cells. *Circulation*. 2000;102(suppl):18.
3. Apfel RE. Acoustic cavitation: a possible consequence of biomedical uses of ultrasound. *Br J Cancer*. 1982;45(suppl):140–146.
4. Maisonhaute E, Prado C, White PC, et al. Surface acoustic cavitation understood via nanosecond electrochemistry, part III: shear stress in ultrasonic cleaning. *Ultrason Sonochem*. 2002;9:297–303.
5. O'Konski MS, White FC, Longhurst J, et al. Ameroid constriction of the proximal left circumflex coronary artery in swine: a model of limited coronary collateral circulation. *Am J Cardiovasc Pathol*. 1987;1:69–77.
6. Roth DM, Maruoka Y, Rogers J, et al. Development of coronary collateral circulation in left circumflex ameroid–occluded swine myocardium. *Am J Physiol*. 1987;253:H1279–1288.
7. Rentrop KP, Cohen M, Blanke H, et al. Changes in collateral channel filling immediately after controlled coronary artery occlusion by an angioplasty balloon in human subjects. *J Am Coll Cardiol*. 1985;5:587–592.
8. Prinzen FW, Bassingthwaighte JB. Blood flow distributions by microsphere deposition methods. *Cardiovasc Res*. 2000;45:13–21.
9. Carmeliet P, Ferreira V, Breier G, et al. Abnormal blood vessel development and lethality in embryos lacking a single VEGF allele. *Nature*. 1996;380:435–439.
10. Ferrara N, Carver-Moore K, Chen H, et al. Heterozygous embryonic lethality induced by targeted inactivation of the VEGF gene. *Nature*. 1996;380:439–442.
11. Isner JM, Pieczek A, Schainfeld R, et al. Clinical evidence of angiogenesis after arterial gene transfer of phVEGF165 in patient with ischaemic limb. *Lancet*. 1996;348:370–374.
12. Baumgartner I, Pieczek A, Manor O, et al. Constitutive expression of phVEGF165 after intramuscular gene transfer promotes collateral vessel development in patients with critical limb ischemia. *Circulation*. 1998;97:1114–1123.
13. Losordo DW, Vale PR, Symes JF, et al. Gene therapy for myocardial angiogenesis: initial clinical results with direct myocardial injection of phVEGF165 as sole therapy for myocardial ischemia. *Circulation*. 1998;98:2800–2804.
14. Asahara T, Murohara T, Sullivan A, et al. Isolation of putative progenitor endothelial cells for angiogenesis. *Science*. 1997;275:964–966.
15. Auge BK, Preminger GM. Update on shock wave lithotripsy technology. *Curr Opin Urol*. 2002;12:287–290.
16. Weil LS Jr, Roukis TS, Weil LS, et al. Extracorporeal shock wave therapy for the treatment of chronic plantar fasciitis: indications, protocol, intermediate results, and a comparison of results to fasciotomy. *J Foot Ankle Surg*. 2002;41:166–172.
17. Fisher AB, Chien S, Barakat AI, et al. Endothelial cellular response to altered shear stress. *Am J Physiol*. 2001;281:L529–L533.
18. Wang FS, Wang CJ, Huang HJ, et al. Physical shock wave mediates membrane hyperpolarization and Ras activation for osteogenesis in human bone marrow stromal cells. *Biochem Biophys Res Commun*. 2001;287:648–655.
19. Gotte G, Amelio E, Russo S, et al. Short-time non-enzymatic nitric oxide synthesis from L-arginine and hydrogen peroxide induced by shock waves treatment. *FEBS Lett*. 2002;520:153–155.
20. Seidl M, Steinbach P, Worle K, et al. Induction of stress fibres and intercellular gaps in human vascular endothelium by shock-waves. *Ultrasonics*. 1994;32:397–400.
21. Wang CJ, Huang HY, Pai CH. Shock wave–enhanced neovascularization at the tendon-bone junction: an experiment in dogs. *J Foot Ankle Surg*. 2002;41:16–22.
22. Millauer B, Wizigmann-Voos S, Schnurch H, et al. High affinity VEGF binding and developmental expression suggest Flk-1 as a major regulator of vasculogenesis and angiogenesis. *Cell*. 1993;72:835–846.

Available online at www.sciencedirect.com
SCIENCE DIRECT
Biosensors and Bioelectronics 20 (2004) 518–523
BIOSENSORS & BIOELECTRONICS
www.elsevier.com/locate/bios

Biocompatible glucose sensor prepared by modifying protein and vinylferrocene monomer composite membrane

Ryoji Kurita[a,*,1], Hisao Tabei[a], Yuzuru Iwasaki[b], Katsuyoshi Hayashi[b], Kenji Sunagawa[c], Osamu Niwa[b]

[a] *NTT Advanced Technology, 3-1 Morinosato-Wakamiya, Atsugi, Kanagawa 243-0198, Japan*
[b] *NTT Microsystem Integration Laboratories, 3-1 Morinosato-Wakamiya, Atsugi, Kanagawa 243-0198, Japan*
[c] *National Cardiovascular Laboratories, 5-7-1 Fujishirodai, Suita, Osaka, 565-8565 Japan*

Received 18 December 2003; received in revised form 25 February 2004; accepted 25 February 2004
Available online 12 April 2004

Abstract

This paper proposes a very simple procedure for preparing a biocompatible sensor based on a protein (bovine serum albumin, BSA), enzyme and vinylferrocene (VF) composite membrane modified electrode. The membrane was prepared simply by first casting vinylferrocene and then coating it with BSA and glucose oxidase immobilised with glutaraldehyde. The sensor response was independent of dissolved oxygen concentration from 3 to 10 ppm and showed good stability for serum sample measurement, unlike the commonly used BSA/enzyme modified electrode. The sensor response was almost unchanged over the measurement time (>10 h) whereas the responses of a BSA and glucose oxidase modified platinum electrode and an osmium-polyvinylpyrridine wired horseradish peroxidase modified electrode (Ohara et al., 1993) fell to 68% of their initial value in a serum sample containing 10 mM glucose.

Keywords: Biocompatibility; Biosensor; Vinylferrocene; In vivo; Glucose

1. Introduction

The real-time monitoring of in vivo biomolecules is important for medical applications such as the measurement of glucose during medical treatment for patients with acute conditions in intensive care units or for the long term monitoring of chronic cases. This might improve the quality of treatment and reduce the number of patient deaths. However, medical analysis has mainly been performed using instruments that employ off-line measurement and this approach takes a relatively long time to provide results.

Various in vivo chemical sensors have been studied with a view to measuring biomolecules in patients continuously and the electrochemical biosensor is an important device for such applications. Two main types of in vivo biosensor have been reported for the continuous in vivo monitoring of biochemicals. One is an on-line biosensor coupled with a microdialysis probe (Ungerstedt, 1986; Lunte et al., 1991; Kurita et al., 2002), the other is a miniaturised biosensor, such as an enzyme modified microelectrode, which is implanted directly in the patient (Abe et al., 1991; Hu et al., 1994; Kissinger et al., 1973). The latter approach is suitable for measuring a localised area with a high temporal resolution. However, the sensitivity of the implanted biosensor decreases due to the adsorption of proteins or thrombus on the sensor surface. Therefore, a stable implantable biosensor is required because it is difficult to calibrate biosensor sensitivity while undertaking a measurement.

Several groups have reported biosensors for stable in vivo measurement that are coated with biocompatible polymers such as cellulose acetate (Fischer et al., 1987), polyethylene glycol (Quinn et al., 1997), polyvinyl chloride (Reddy and Vadgama, 1997), polyurethane (Ishihara et al., 1995) and Nafion (Turner et al., 1990). Surface modification with commercially available polymers has been widely used for various sensors due to its simplicity. Reddy and Vadgama (1997) studied the variation in lactate sensor response with time in whole blood. They reported that a polyvinyl chloride coating is useful for stable in vivo monitoring. Although

* Corresponding author. Tel.: +81-46-240-3538; fax: +81-46-240-4728.
E-mail address: kurita@atsugi.ntt-at.co.jp (R. Kurita).
[1] Tel.: +81-46-240-3538; fax: +81-46-240-4728

0956-5663/$ – see front matter © 2004 Elsevier B.V. All rights reserved.
doi:10.1016/j.bios.2004.02.018

this method led to a quantitative improvement of biosensors in blood, it remains unsatisfactory because the sensitivity of the initial response decreased to about 60% after 6 h in blood. Kros et al. (2001) compared biocompatible coatings on a glucose sensor by using heparin, polyethylene glycol, dextran, Nafion and polystyrene in serum and albumin solution. They reported that the responses of the glucose sensors with these polymers were improved compared with that of a non-coated sensor in serum. However, the sensitivity of these sensors decreased to less than half the initial response in serum after a few hours. Moreover, oxygen free measurement is required for in vivo biosensors since the in vivo oxygen concentration is changeable. Therefore, we need to modify the mediator to enable it to communicate between enzyme and electrode if we are to fabricate in vivo biosensors.

Since in vivo biosensors require a biocompatible membrane and an enzyme membrane with high electron transfer between enzyme and electrode, it is more convenient if the membrane has both biocompatibility and electron conductivity. Inoue et al. (2002) reported a polypyrrole derivative-based glucose sensor fabricated by the electropolymerisation of 1-(6-D-gluconamidohexyl) pyrrole. They reported that the electropolymerised membrane prevented plasma from being absorbed by the sensing membrane in the blood sample. It is easy to obtain a common monomer such as *o*-phenylenediamine and realise a selective membrane. However, it requires sophisticated organic synthesis skills to prepare monomers with which to obtain biocompatible and electroconductive polymers by electrochemical polymerisation and the polymerisation conditions must also be optimised without losing enzyme activity.

In this paper, we propose a new procedure for preparing glucose biosensors for in vivo monitoring based on a composite enzyme membrane composed of mediator and protein. The sensor membrane consists of vinylferrocene and bovine serum albumin (BSA) in which glucose oxidase is immobilised with glutaraldehyde and this sensor shows improved stability for serum sample measurement.

2. Experimental

2.1. Chemicals

Vinylferrocene (VF) and BSA were purchased from Aldrich (Steinheim, Germany). Glucose oxidase (GOD) was purchased from Sigma Chemical Co. (St. Louis, MO, USA). Glutaraldehyde and glucose were purchased from Kanto Chemicals (Tokyo, Japan). Phosphate buffered saline (PBS; pH 7.4) was purchased from Life Technology (Grand Island, NY). Osmium-polyvinylpyridine wired horseradish peroxidase (Ohara et al., 1993; Os-gel-HRP) was purchased from Bioanalytical Systems (West Lafayette, IN).

2.2. Sensor fabrication

The glucose sensor was fabricated using a 1.6 mm diameter Pt electrode (BAS). We polished the Pt electrode on a polishing paper impregnated with 1 μm diamond particles, and rinsed it with pure water. We then immersed the electrode in 0.7 μl/mm^2 of 0.3 M VF in methanol and dried it. Next, we modified the VF modified Pt electrode with 1.4 μl/mm^2 of GOD solution. The GOD solution contained 0.37 U/μl of GOD, 2% albumin and 0.5% glutaraldehyde.

We fabricated two conventional sensors for comparison with our sensor, one was a Pt electrode modified with GOD and albumin cross-linked with glutaraldehyde (Yao, 1983; Guilbault and Lubrano, 1973), the other was an Os-gel-HRP-based glucose sensor as described previously (Ohara et al., 1993). The electrode area and amount of modified GOD, albumin and glutaraldehyde were the same as those of the VF-based sensor.

2.3. Measurements

Cyclic voltammetry and amperometric measurements were performed using an electrochemical analyser (CH Instruments model 1000, Austin, TX). An Ag/AgCl reference electrode (Bioanalytical Systems) and a Pt wire auxiliary electrode were used. In cyclic voltammetry, the potential of the working electrode was scanned from 0 to 0.6 V at a scan rate of 2 mV/s and the buffer solutions were argon or air saturated for 10 min before the measurement. In the amperometric measurement, the potential of the working electrode of the VF-based sensor was held at 0.3 V. The conventional Pt electrode sensor modified with GOD and the Os-gel-HRP-based sensor were held at 0.5 and 0 V, respectively. The buffer solutions were air saturated and stirred gently with a magnetic bar. All measurements were performed at room temperature.

X-ray photoelectron spectroscopy (XPS) was performed using a Kratos AXIS Ultra (AlKR1846.6 eV) spectrometer to determine the elemental composition of the sensing membrane surface.

3. Results and discussion

Fig. 1 shows cyclic voltammograms (CV) of our glucose sensor in (a) 1 mM glucose solution and (b) PBS without glucose. CV (b) shows the anodic and cathodic peaks of the electrode modified with VF. The anodic current increases with increasing potential, and reaches a plateau above 50 nA as shown in CV (b). In contrast, CV (a) for a 1 mM glucose solution shows a higher anodic current (about 0.45 μA) than that of CV (b) and the cathodic current has disappeared. The higher anodic electrocatalytic current in the presence of glucose without oxygen in the sample suggests that there was an electron transfer between VF and GOD. The VF must disperse in the membrane to transfer electrons directly

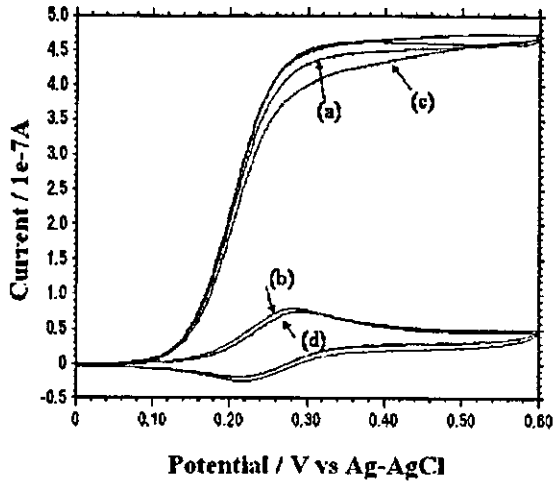

Fig. 1. Cyclic voltammograms at a platinum electrode modified with a composite enzyme membrane composed of vinylferrocene, glucose oxidase and bovine serum albumin. (a) In 1 mM glucose solution without oxygen; (b) in PBS without glucose without oxygen; (c) in 1 mM glucose solution with oxygen and (d) in PBS without glucose with oxygen.

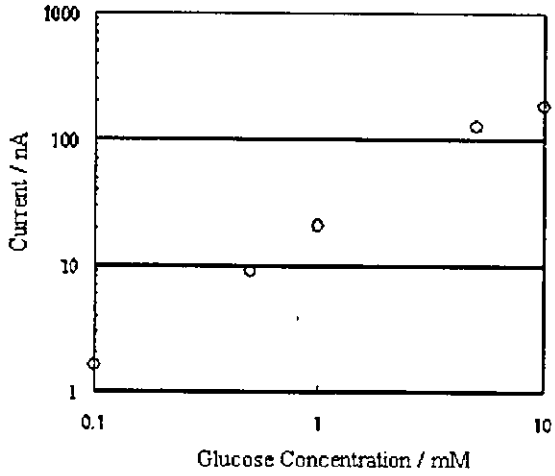

Fig. 3. Calibration curve of the vinylferrocene-based glucose sensor. The potential of the working electrode was kept at 0.3 V vs. Ag/AgCl.

between the electrode and enzymes, and so we studied the VF distribution by measuring iron atoms with XPS.

Fig. 2 shows a typical XPS spectrum of the membrane of the VF-based glucose sensor. The spectrum shows carbon, nitrogen and oxygen peaks, which can be attributed to albumin. In contrast, we observed no peaks for the Pt electrode because XPS provides an analysis that reaches only a few tens of nanometers below the surface. However, we observed small iron peaks attributable to VF. These peaks indicate that VF molecules are distributed throughout all of the BSA film. This also suggests the possibility of electron transfer between GOD and VF since there are VF molecules near the GOD and electron transfer might take place as a result of the electrons hopping through the VF in the film or by the diffusion of the VF itself in the film.

Fig. 3 shows the calibration curve of our glucose sensor. The PBS was air saturated and we measured the steady-state anodic current at 0.3 V. The anodic current of the sensor exhibited good linearity with the glucose concentration between 0.1 and 10 mM. However, the anodic current of the sensor saturated when the concentration was above 10 mM. It is known that the hydrogen peroxide detection type glucose sensor reaches saturation when the glucose concentration is higher than a few mM (Harrison et al., 1988). This is because the sensitivity is affected by the concentration of dissolved oxygen in the buffer solution. However, we have already confirmed that our sensor works without oxygen

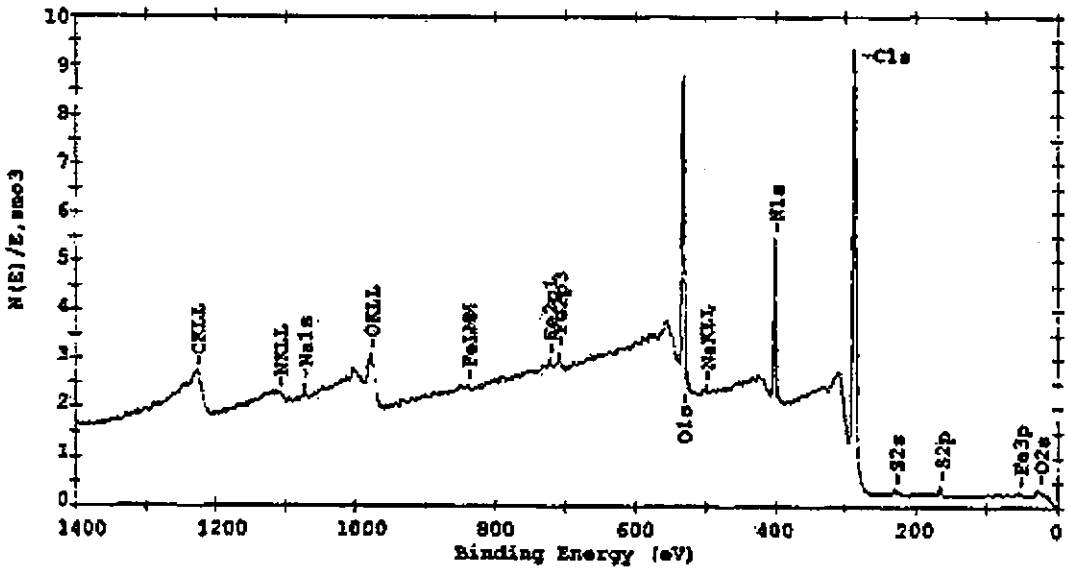

Fig. 2. XPS spectrum of the sensing membrane on the VF-based glucose sensor.

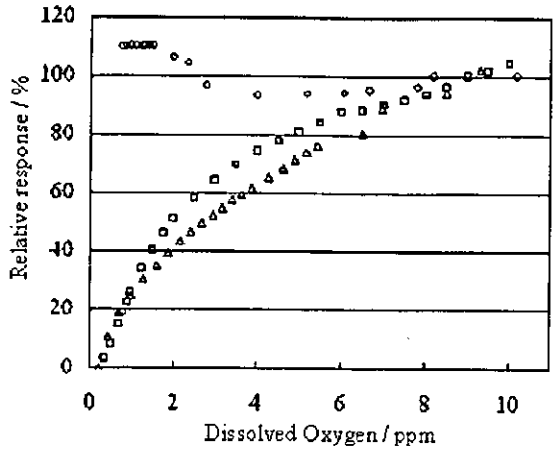

Fig. 4. Variations in the current response with changes in the dissolved oxygen concentration obtained using the vinylferrocene-based glucose sensor (circles), the conventional glucose sensor without mediators (squares) and the Os-gel-HRP-based glucose sensor (triangles). The electrodes were kept at 0.3, 0.5 and 0 V vs. Ag/AgCl, respectively.

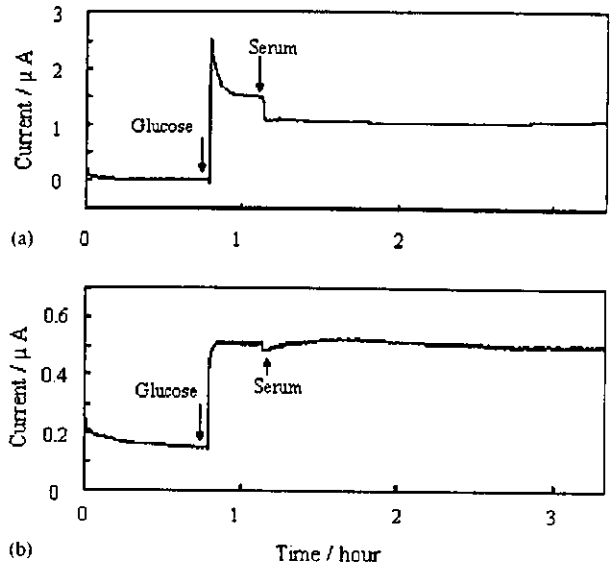

Fig. 5. Variation in the current response to 10 mM glucose with and without 10% horse serum obtained using (a) the conventional glucose sensor and (b) the vinylferrocene-based glucose sensor.

as shown in Fig. 1. Cass et al. (1984) reported an electron transfer between ferrocene derivatives and GOD. They measured the CV in a glucose solution containing GOD using a ferrocene derivative modified electrode. Their CV shows a faster anodic catalytic current than our CV in Fig. 1(a). We considered the reason for the slower electron transfer of our sensor to be as follows. With the sensor reported by Cass et al. (1984), the ferrocene derivatives were immobilised with a relatively high density on the electrode and GOD could diffuse freely in the solution. Therefore, the electron transfer between GOD and the electrode takes place via the ferrocene derivatives, which are immobilised with a high density on the surface.

In contrast, in our case GOD is covalently bonded in the BSA film, and so the electron transfer between GOD and the electrode should be achieved by VF diffusion in the film or electron hopping from GOD and the electrode through many VF molecules. The slower electron transfer of our system is because the VF diffusion is slower in the film than in the solution and the VF density in our sensor film is lower than the surface ferrocene concentration reported by Cass et al. (1984).

However, we were still able to achieve a high current density since the total amount of VF and GOD is much greater than those of the sensor reported by Cass et al. (1984), since our film is much thicker.

Fig. 4 shows the variations in the current responses of the VF-based sensor (circles), a conventional glucose sensor consisting of a Pt electrode modified with GOD and albumin cross-linked with glutaraldehyde (Yao, 1983; Guilbault and Lubrano, 1973) (squares) and an electrode modified with a mediator (Os-gel-HRP) (triangles) to a 10 mM glucose solution when we changed the dissolved oxygen concentration. We held the potentials for the VF based and conventional sensors at 0.3 and 0.5 V versus Ag/AgCl, respectively. In contrast, we held the Os-gel-HRP-based sensor at 0 V versus Ag/AgCl during the measurement. Each relative response was defined by dividing the currents obtained at various oxygen concentrations by the current when the dissolved oxygen concentration was 9 ppm in the form of air saturated oxygen concentration at room temperature. The electrode area and amount of modified GOD, albumin and glutaraldehyde were the same as those of the VF-based sensor. We modified the Os-gel-HRP-based glucose sensor as described previously (Ohara et al., 1993). The current responses of the glucose sensor without the mediator and the Os-gel-HRP-based glucose sensor decreased as the dissolved oxygen decreased because there was insufficient oxygen to deoxidise GOD in PBS. This reveals the usual problem with hydrogen peroxide detection type electrochemical biosensors when used for in vivo monitoring. In contrast, the VF-based glucose sensor showed an almost steady response of 93–100% when the dissolved oxygen concentration was changed between 3 and 10 ppm. The responses at the VF-based glucose sensor increased when the dissolved oxygen concentration was less than 3 ppm. This is because only direct electron transfer between the enzyme and electrode through VF takes place when the dissolved oxygen concentration is sufficiently low. Although the sensitivity of the VF-based sensor changed at low dissolved oxygen concentrations, this is not a serious problem for in vivo monitoring in blood because the dissolved oxygen concentration in blood is about 4–5 ppm.

Fig. 5(a and b) show the responses of the two types of sensors to a 10 mM glucose solution. Fig. 5(a) shows the current variation at a conventional glucose sensor with a Pt electrode modified with GOD and albumin cross-linked with glutaraldehyde (Yao, 1983; Guilbault and Lubrano, 1973). Fig. 5(b) shows the current variation at the VF-based

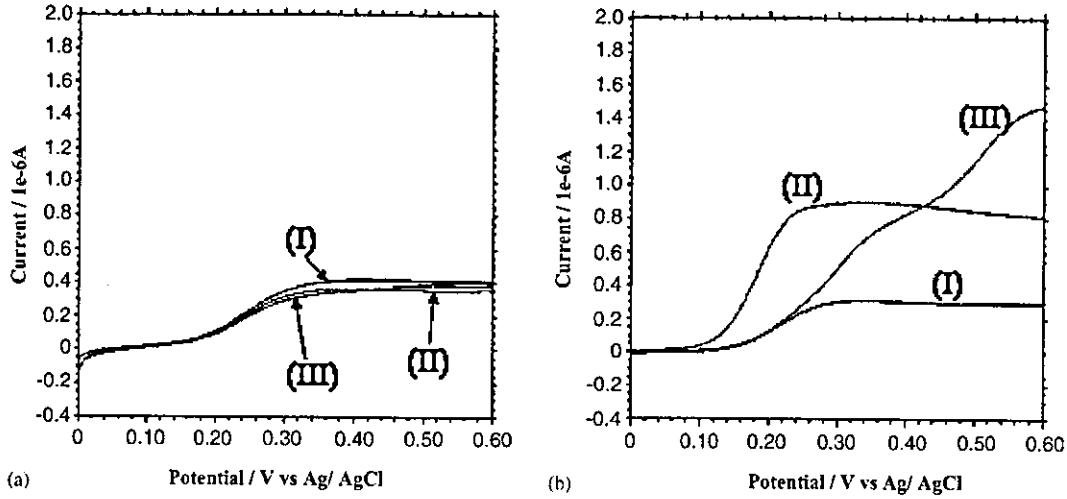

Fig. 6. Linear sweep voltammograms with VF-based sensor (a) with (b) without Nafion membrane in (I) 1 mM glucose, (II) 1 mM glucose with 1 mM ascorbic acid, (III) 1 mM glucose with 1 mM uric acid.

glucose sensor described in this report. The PBS was air saturated and stirred gently with a magnetic bar. The potential of the conventional and VF-based electrodes were kept at 0.5 and 0.3 V, respectively. After we observed that the 10 mM glucose current was stable for 30 min, we injected PBS containing horse serum into the sample solution until the serum concentration in the sample solution reached 10%. When we added the horse serum, the anodic current immediately decreased to 68% of its initial response. This current reduction resulted from the adsorption of proteins in the serum onto the surface of the sensing membrane and this reduced the diffusion of the glucose into the membrane. The reduced current did not recover for 10 h after we placed the electrode in PBS containing horse serum. Furthermore, we observed no current increase when we measured a 10 mM glucose solution containing no serum using a sensor that had already been placed in serum once and had then been rinsed with PBS. Fig. 5(b) also shows the current increase at the VF-based glucose sensor that resulted from adding 10 mM glucose. In contrast, we observed no current decrease, except for a slight current fluctuation when we added the serum to the sample, until the serum concentration reached 10%. This suggests that our sensing membrane exhibits good resistance to protein fouling. This also indicates that our sensor is suitable for the quantitative in vivo monitoring of glucose concentration. We observed no current reduction for more than 10 h. The current reduction after 10 h was due to the reduction of VF on the electrode. It is known that ferrocene is converted to ferrocium ions when it is electrochemically oxidised on the electrode. So oxidised VF could become easily detached from an electrode into a bulk solution since hydrophilicity increases after oxidation. We overcoated a Nafion membrane onto the sensing membrane to trap ferricinium ions (cations) since Nafion is an anionic polymer. After the sensor was coated with Nafion, its response remained unchanged for 3 days in buffer solution. Although the sensitivity of a glucose sensor coated with Nafion film is stable compared with that of an uncoated sensor, Kros et al. (2001) reported that the sensitivity decreased to about 40% of its initial response in serum after a few hours (Kros et al., 2001). Our VF-based glucose sensor exhibited much greater stability even after it was modified with Nafion film. The magnitude of the current was almost the same after 3 days of measurement. This improved stability might be due to the stability of the bottom layer, which consists of VF/BSA composite film.

In addition, the sensor also showed selectivity to L-ascorbic acid and uric acid, which are typical interferents for in vivo measurement. Fig. 6 shows the results of linear sweep voltammograms of the VF-based sensor (a) with (b) without a Nafion membrane in 1 mM glucose with 1 mM ascorbic acid or 1 mM uric acid. Fig. 6(b) shows that the anodic current in 1 mM glucose with ascorbic acid or uric acid is higher than that without the acid (interference). This indicates that it is difficult to measure the glucose concentration quantitatively since the oxidation potential of VF is close to that of ascorbic acid and uric acid. However, Fig. 6(a) shows that the current responses of the sensor in 1 mM glucose containing ascorbic acid or uric acid are almost the same as those for 1 mM glucose without interference. This is because Nafion is capable of rejecting anions that include ascorbic acid and uric acid by electrostatic repulsion.

4. Conclusion

We used a new simple preparation procedure to develop a biocompatible glucose biosensor based on a composite enzyme membrane consisting of vinylferrocene and glucose oxidase. The sensor response was independent of the dissolved oxygen concentration between 3 to 10 ppm and

showed a stable response in serum for 10 h. The sensor also shows good selectivity to ascorbic acid or uric acid when it is overcoated with a Nafion membrane. The sensor could be employed for quantitative in vivo monitoring.

Acknowledgements

The authors thank Drs. N. Yabumoto, M. Hikita and H. Ichino for encouraging this project and Dr. H. Ando for assistance with the XPS measurement. This project received financial support from the New Energy and Industrial Technology Development Organization in Japan.

References

Abe, T., Lau, Y.Y., Ewing, A.G., 1991. Intracellular analysis with an immobilized- enzyme glucose electrode having a 2-pm diameter and subsecond response times. J. Am. Chem. Soc. 13, 7421–7423.

Cass, A.E.G., Davis, G., Francis, G.D., Hill, H.A.O., Aston, W.J., Higgins, I.J., Plotkin, E.V., Scott, L.D.L., Turner, A.P.F., 1984. Ferrocene-mediated enzyme electrode for amperometric determination of glucose. Anal. Chem. 56, 667–671.

Fischer, U., Ertle, R., Abel, P., Rebrin, K., Brunstein, E., Hahn von Dorsche, H., Freyse, E.J., 1987. Assessment of subcutaneous glucose concentration: validation of the wick technique as a reference for implanted electrochemical sensors in normal and diabetic dogs. Diabetologia 30, 940–945.

Guilbault, G.G., Lubrano, G.J., 1973. An enzyme electrode for the amperometric determination of glucose. Anal. Chim. Acta 64, 439–455.

Harrison, D.J., Turner, R.F.B., Baltes, H.P., 1988. Characterization of perfluorosulfonic acid polymer coated enzyme electrodes and a miniaturized integrated potentiostat for glucose analysis in whole blood. Anal. Chem. 60, 2002–2007.

Hu, Y., Michel, K.M., Albahadily, F.N., Michaels, E.K., Wilson, G.S., 1994. Direct measurement of glutamate release in the brain using a dual enzyme-based electrochemical sensor. Brain Res. 659, 117–125.

Inoue, S., Yasuzawa, M., Imai, S., 2002. Preparation of glucose sensor using organopolysiloxane/polypyrrole complex film. Chem. Sens. Suppl. A 18, 136–138.

Ishihara, K., Hanyuda, H., Nakabayashi, N., 1995. Synthesis of phospholipid polymers having a urethane bond in the side chain as coating material on segmented polyurethane and their platelet adhesion-resistant properties. Biomaterials 16, 873–879.

Kissinger, P.T., Hart, J.B., Adams, R.N., 1973. Voltammetry in brain tissue—a new neurophysiological measurement. Brain Res. 55, 209–213.

Kros, A., Gerritsen, M., Sprakel, V.S.I., Sommerdijk, N.A.J.M., Jansen, J.A., Nolte, R.J.M., 2001. Silica-based hybrid materials as biocompatible coatings for glucose sensors. Sens. Actuators B 81, 68–75.

Kurita, R., Hayashi, K., Fan, X., Yamamoto, K., Kato, T., Niwa, O., 2002. Microfluidic device integrated with pre-reactor and dual enzyme modified microelectrodes for monitoring in vivo glucose and lactate. Sens. Actuators B 87, 296–303.

Lunte, C.E., Scott, D.O., Kissinger, P.T., 1991. Sampling living systems using microdialysis probes. Anal. Chem. 63, 773A–780A.

Ohara, T.J., Vreeke, M.S., Battaglini, F., Heller, A., 1993. Preparation of bienzyme sensors with "electrically wired" peroxidase. Electroanalysis 5, 825–831.

Quinn, C.A.P., Connor, R.E., Heller, A., 1997. Biocompatible glucose-permeable hydrogel for in situ coating of implantable biosensors. Biomaterials 18, 1665–1670.

Reddy, S.M., Vadgama, P.M., 1997. Surfactant-modified poly(vinyl chloride) membranes as biocompatible interfaces for amperometric enzyme electrodes. Anal. Chim. Acta 350, 77–89.

Turner, R.F., Harrison, D.J., Rajotte, R.V., Baltes, H.P., 1990. A biocompatible enzyme electrode for continuous in vivo glucose monitoring in whole blood. Sens. Actuators B1, 561–564.

Ungerstedt, U., 1986. Microdialysis—a new bioanalytical sampling technique. Curr. Sep. 7, 43–46.

Yao, T., 1983. A chemically-modified enzyme membrane electrode as an amperometric glucose sensor. Anal. Chim. Acta 148, 27–33.

Blockade of Vascular Endothelial Growth Factor Suppresses Experimental Restenosis After Intraluminal Injury by Inhibiting Recruitment of Monocyte Lineage Cells

Kisho Ohtani, MD; Kensuke Egashira, MD, PhD; Ken-ichi Hiasa, MD; Qingwei Zhao, MD; Shiro Kitamoto, MD; Minako Ishibashi, MD; Makoto Usui, MD; Shujiro Inoue, MD; Yoshikazu Yonemitsu, MD; Katsuo Sueishi, MD; Masataka Sata, MD; Masabumi Shibuya, MD; Kenji Sunagawa, MD

Background—Therapeutic angiogenesis by delivery of vascular endothelial growth factor (VEGF) has attracted attention. However, the role and function of VEGF in experimental restenosis (neointimal formation) after vascular intraluminal injury have not been addressed.

Methods and Results—We report herein that blockade of VEGF by soluble VEGF receptor 1 (*sFlt-1*) gene transfer attenuated neointimal formation after intraluminal injury in rabbits, rats, and mice. *sFlt-1* gene transfer markedly attenuated the early vascular inflammation and proliferation and later neointimal formation. *sFlt-1* gene transfer also inhibited increased expression of inflammatory factors such as monocyte chemoattractant protein-1 and VEGF. Intravascular VEGF gene transfer enhanced angiogenesis in the adventitia but did not reduce neointimal formation.

Conclusions—Increased expression and activity of VEGF are essential in the development of experimental restenosis after intraluminal injury by recruiting monocyte-lineage cells. **(*Circulation*. 2004;110:2444-2452.)**

Key Words: restenosis ■ remodeling ■ inflammation ■ endothelium-derived factors ■ gene therapy

Vascular endothelial growth factor (VEGF) has attracted attention for endothelial regeneration and angiogenesis.[1–3] VEGF is one of the most potent vascular permeability factors known, is thought to function as an endogenous regulator of endothelial integrity after injury, and thus, protects the artery from disease progression.[4] Previous animals studies have reported that local delivery of VEGF after endothelial injury promotes endothelial regeneration, accelerates the recovery of endothelium-dependent relaxation, and reduces neointimal formation (see review[4]), suggesting the close correlation between accelerated endothelial integrity and reduced neointima after balloon injury. Increased expression of VEGF and its 2 receptors (VEGFR-1, Flt-1; VEFGR-2, Flk-1) in atherosclerotic and restenotic lesions has been reported.[5–7] However, there is still considerable debate over the vasculoprotective versus atherogenic effects of VEGF.[8] Emerging evidence suggests that (1) VEGF induces migration and activation of monocytes[9]; (2) VEGF induces adhesion molecules[10] and monocyte chemoattractant protein-1 (MCP-1)[11]; and (3) VEGF enhances neointimal formation and atherogenesis by stimulating intraplaque angiogenesis in hypercholesterolemic animals without balloon injury[12,13] or by increasing monocyte infiltration into atherosclerotic lesions.[14] Therefore, it remains unclear whether VEGF protects the artery from vascular disease or accelerates vascular disease.

See p 2283

Clinical and experimental studies involving arterial gene transfer of VEGF showed that it failed to reduce restenosis after balloon angioplasty.[15–17] The role of VEGF in restenotic changes (neointimal formation and negative remodeling) after injury therefore remains a mystery. This is mainly because the inhibitor of VEGF has not been tested for experimental restenosis, although inhibitors of VEGF are currently being evaluated for tumor angiogenesis and other treatment-intractable inflammatory disorders.[3] It is practically impossible to investigate the role of VEGF in postnatal life in mice lacking VEGF or its receptors, because the absence of VEGF function leads to embryonic lethality owing to vascular defects.[4] A soluble form of the VEGF receptor-1 (sFlt-1) is expressed endogenously by vascular endothelial cells and can inhibit VEGF activity by directly sequestering VEGF and by functioning as a dominant-negative inhibitor against VEGF.[18] We and others have demonstrated that intramuscular transfection of the *sFlt-1* gene effectively and specifically

Received June 18, 2004; revision received August 14, 2004; accepted August 20, 2004.

From the Departments of Cardiovascular Medicine (K.O., K.E., M.U., Q.Z., S.K., M.I., K.-i.H., S.I., K.S.) and Pathology (Y.Y., S.K.), Graduate School of Medical Sciences, Kyushu University, Fukuoka; the Department of Cardiovascular Medicine (M. Sata), Graduate School of Medical Sciences, University of Tokyo, Tokyo; and the Division of Genetics (M. Shibuya), Institute of Medical Science, University of Tokyo, Tokyo, Japan.

An online-only Data Supplement is available at http://www.circulationaha.org

Correspondence to Kensuke Egashira, MD, PhD, Department of Cardiovascular Medicine, Graduate School of Medical Science, Kyushu University, 3-1-1, Maidashi, Higashi-ku, Fukuoka 812-8582, Japan. E-mail egashira@cardiol.med.kyushu-u.ac.jp

Circulation **is available at http://www.circulationaha.org** **DOI: 10.1161/01.CIR.0000145123.85083.66**

blocks VEGF and thus, "quenches" the activity of VEGF in remote organs in vivo.[19,20]

The aim of this study was to decisively determine a role for VEGF in restenotic changes after intraluminal injury. We report herein that blockade of VEGF by systemic *sFlt-1* gene transfer attenuates the development of neointimal formation after intraluminal injury by inhibiting inflammation, which suggests an essential role for VEGF in the pathogenesis of restenosis after injury. Our present data are clinically important because VEGF gene therapy for therapeutic angiogenesis and restenosis has been attempted in clinical studies.[16,17,21]

Methods

Expression Vector

The 3.3-kb mouse *sFLT-1* gene, originally obtained from the mouse lung DNA library,[22] was cloned into the *Bam*HI (5′) and *Not*I (3′) sites of the eukaryotic expression vector plasmid cDNA3 (Invitrogen). Plasmid cDNA3 encoding the luciferase gene was used to detect gene transfection.

Rat and Rabbit Models of Balloon Injury

The study protocol was reviewed and approved by the Committee on Ethics on Animal Experiments, Kyushu University Faculty of Medicine, and the experiments were conducted according to the guidelines of American Physiological Society. A portion of this study was performed at the Kyushu University Station for Collaborative Research.

Twenty-week-old male, normal chow–fed Wistar-Kyoto rats were anesthetized, and their right common carotid arteries were injured by passage (3 times) of an infiltrated 2F Fogarty balloon catheter.[23] Male Japanese white rabbits weighing 3.0 to 3.5 kg were fed a high-cholesterol diet for 2 weeks. Their right common carotid arteries also were injured by passage (3 times) of an inflated 2F Fogarty catheter.[24] After injury, all rabbits were fed the same high-cholesterol diet. Three days before balloon injury, the animals were randomly divided into 2 groups: the empty-plasmid group was injected with the empty plasmid, and the *sFlt-1* group was injected with the *sFlt-1* gene into femoral muscle (150 μg/50 μL TE buffer [10 mmol/L Tris-HCl, 1 mmol/L EDTA, pH 8.0] in rats, 1500 μg/0.5 mL TE buffer in rabbits). To enhance transgene expression, all plasmid-injected animals received electroporation at the injection site immediately after injection with an electric pulse generator (CUY21, BTX) as previously described.[19,23–25]

Morphometric and Immunohistochemical Analyses

All animals were euthanized by intravenous injection of a lethal dose of sodium pentobarbital. Tissue sections from rabbits and rats were prepared as described[23,24] and either (1) stained with Masson's trichrome or elastica van Gieson's stains or (2) subjected to immunostaining with antibodies against macrophages/monocytes (ED1, Serotec, for rats; RAM11, Dako, for rabbits), proliferating cells (proliferating cell nuclear antigen for rats from Dako, Ki-67 for rabbits from Dako), endothelial cells (CD31, Dako), VEGF (Santa Cruz), VEGFR-1 (Santa Cruz), VEGFR-2 (Santa Cruz), α-smooth muscle actin (Dako), MCP-1 (R&D Systems), interleukin-1β (IL-1β; R&D Systems), or nonimmune mouse IgG (Zymed). After avidin-biotin amplification, the slides were incubated with diaminobenzidine and counterstained with hematoxylin. Immunofluorescence double staining was performed to localize VEGF and its receptors by the use of fluorescence-conjugated antibodies in rats. Morphometric analysis was performed by microscopy with a computerized digital image-analysis system by a single observer who was blinded to the treatment protocol.[23,24]

Real-Time Quantitative Reverse Transcription–PCR

Real-time polymerase chain reaction (PCR) amplification was performed with rabbit cDNA by using the ABI PRISM 7000 sequence detection system (Applied Biosystems) as described previously.[23] The respective PCR primers and TaqMan probes were designed from GenBank databases aided by a software program (Applied Biosystems; online Table I). Results were analyzed by sequence detection software (Applied Biosystems), expressed in arbitrary units, and adjusted for glyceraldehyde 3-phosphate dehydrogenase mRNA levels.

Mouse Femoral Wire-Injury Model With Bone Marrow Reconstitution

Intraluminal injury of the femoral artery of wild-type mice whose bone marrow had been replaced with that of ROSA26 mice, which expresses β-galactosidase (LacZ) ubiquitously, was performed.[26] Four weeks after bone marrow transplantation, transluminal arterial injury was induced by inserting a straight spring wire (0.38 mm in diameter) into the femoral artery as described.[26] The femoral artery was excised and stained with X-gal solution for 7 hours and then fixed in 4% paraformaldehyde. LacZ-positive cells were counted and expressed as a proportion of the total number of cells. The paraffin-embedded sections were stained with elastica van Gieson's stain.

Peripheral blood was obtained from the retro-orbital venous plexus of the mice. Fluorescence-conjugated antibodies against CD31 (Pharmingen) and c-Kit (Pharmingen) were used as bone marrow–derived monocyte-lineage markers. A fluorescein isothiocyanate–conjugated antibody against Mac-1 (Pharmingen) was used as a circulating monocyte-lineage marker after gating for monocyte cell size with exclusion of granulocytes. Data were analyzed by flow cytometry and appropriate software (Becton Dickinson).

Blood Measurements

Plasma total cholesterol levels in rabbits were determined with commercially available kits (Wako Pure Chemicals). To measure sFlt-1 released by the transfected skeletal muscle, plasma concentrations of sFlt-1 were measured by use of an sFlt-1 ELISA kit (R&D Systems) in rabbits. Concentrations of VEGF in plasma and femoral arterial tissues were also measured in mice by use of an ELISA kit (R&D Systems).

Statistical Analysis

Data are expressed as mean±SE. Statistical analysis of differences was compared by ANOVA and Bonferroni's multiple-comparison tests. A level of $P<0.05$ was considered statistically significant.

Results

Increased Expression of VEGF and Its Receptors in Rabbits and Rats

Significant increases in VEGF mRNA levels were detected after balloon injury in rabbits, which peaked on day 7 and persisted until day 28 (Figure 1A). Immunohistochemical staining revealed that VEGF and VEGFR-1 increased in vascular smooth muscle cells in the media and regenerated endothelial layer during the early phase (day 7) and in cells in the neointima, media, and adventitia during the later phase (day 28) after balloon injury in rabbits (Figure 1B). VEGFR-2 did not increase on day 7 but did increase in the injured artery on day 28. *sFlt-1* gene transfer reduced the increased immunoreactivities of VEGF, VEGFR-1, and VEGFR-2 on day 28 (Figure 1B).

The localization of VEGF, VEGFR-1, and VEGFR-2 was studied in rats by immunohistochemistry. As observed in rabbits, immunoreactive VEGF and VEGFR-1 increased in the media on days 3 and 7 and in the neointima, media, and adventitia on day 28 (Figure 2A). The increase in immunoreactive VEGFR-2 was less prominent during the early phase but became apparent on day 28 (Figure 2A).

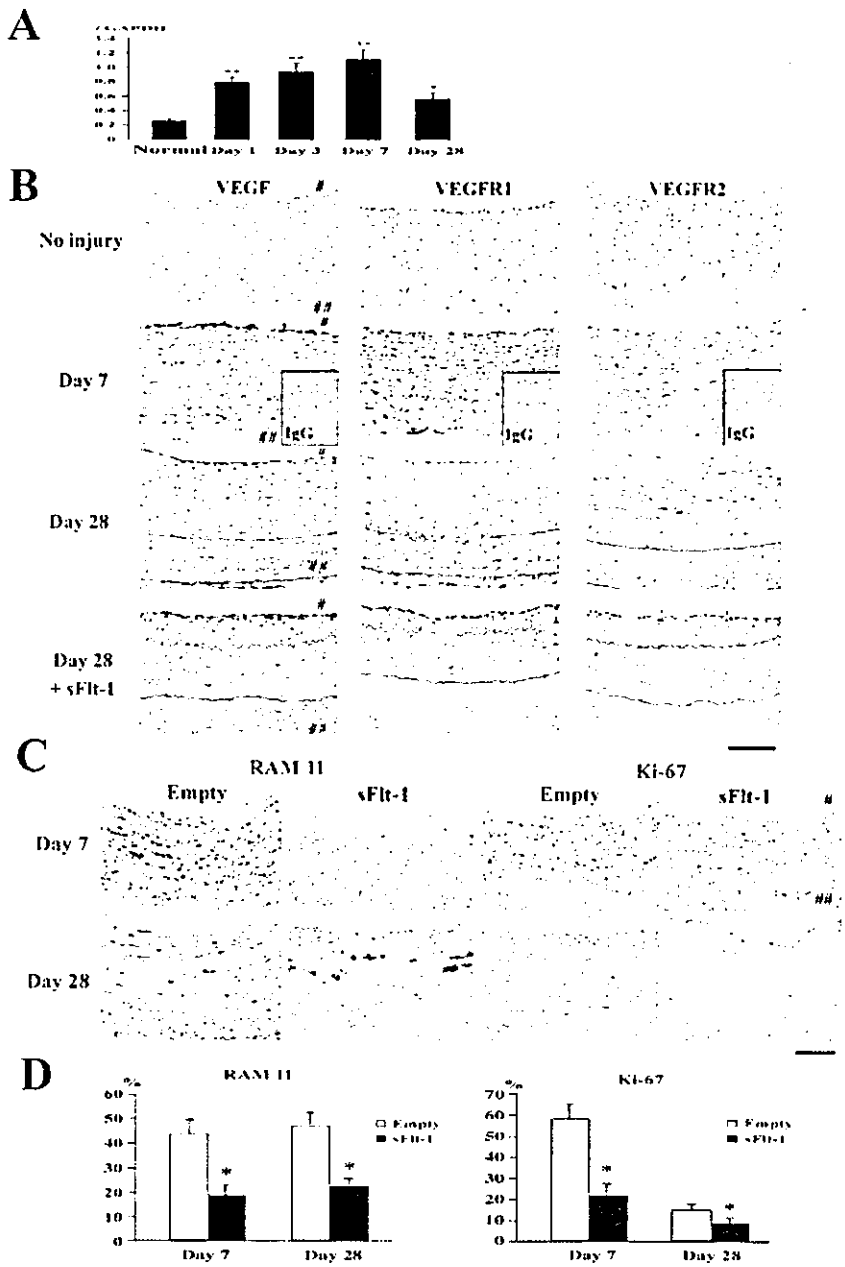

Figure 1. Expression of VEGF after balloon injury and inhibitory effects of *sFlt-1* gene transfer on inflammatory-proliferative changes in rabbits. A, Time course of VEGF mRNA levels in rabbits. mRNA levels were assessed by real-time PCR at indicated times. Expression of VEGF mRNA in each sample was normalized to glyceraldehyde 3-phosphate dehydrogenase mRNA expression in that sample. Each bar has n=6 to 8. $^{*}P<0.05$, $^{**}P<0.01$ vs control (uninjured) artery. B, Immunohistochemistry of rabbit carotid artery. Arterial cross sections were stained immunohistochemically with VEGF, VEGFR-1 (Flt-1), VEGFR-2 (Flk-1), or nonimmune IgG. # and ## indicate lumen and adventitia, respectively. Internal and external elastic layers are highlighted with blue and black lines, respectively, in photographs taken 28 days after injury. Bar indicates 100 μm. C, Carotid artery sections from empty-plasmid and *sFlt-1* groups 7 and 28 days after balloon injury were stained immunohistochemically with antibody against monocytes/macrophages (RAM11) or proliferating cells (Ki-67). # and ## indicate lumen and adventitia, respectively. Bar=100 μm. D, Effect of *sFlt-1* gene transfer on inflammation (RAM11-positive monocytes/macrophages) and proliferation (Ki-67–positive cells) 7 and 28 days after balloon injury (n=8 each). $^{*}P<0.01$ vs control group.

Fluorescence double immunohistochemistry revealed that VEGF and VEGFR-1 were expressed predominantly in α-smooth muscle actin–positive cells in the media and neointima on day 28 (Figure 2B). During the early phase, ED1-positive monocytes recruited into the intima and adventitia expressed VEGFR-1 but not VEGFR-2 (Figure 2C). *sFlt-1* gene transfer reduced the increased immunoreactivities of VEGF, VEGFR-1, and VEGFR-2 on day 28 (data not shown).

Inhibitory Effects of *sFlt-1* Transfer on Inflammatory and Proliferative Changes in Rabbits

As we reported,[23,24] inflammatory and proliferative changes became evident by 3, 7, and 28 days after balloon injury in rabbits (Figure 1C and 1D). *sFlt-1* gene transfer reduced these inflammatory and proliferating changes.

Inhibitory Effects of *sFlt-1* Transfer on Neointimal Formation and/or Negative Remodeling in Rabbits and Rats

The carotid arteries in the control and empty-plasmid groups developed significant neointimal formation and negative remodeling (smaller lumen size, internal elastic lamina, and external elastic lamina) in rabbits by day 28 (Figure 3A and 3B). The arteries from the *sFlt-1* group showed less neointimal formation, negative remodeling, perivascular fibrosis, and adventitial vasa vasorum; an adventitial VEGFR-2–positive vasa vasorum; and a larger lumen area. There was no significant difference in plasma levels of total cholesterol between the 2 groups (online Table II), indicating that the observed effects of *sFlt-1* gene transfer were not caused by changes in serum cholesterol levels. In rats, neointimal

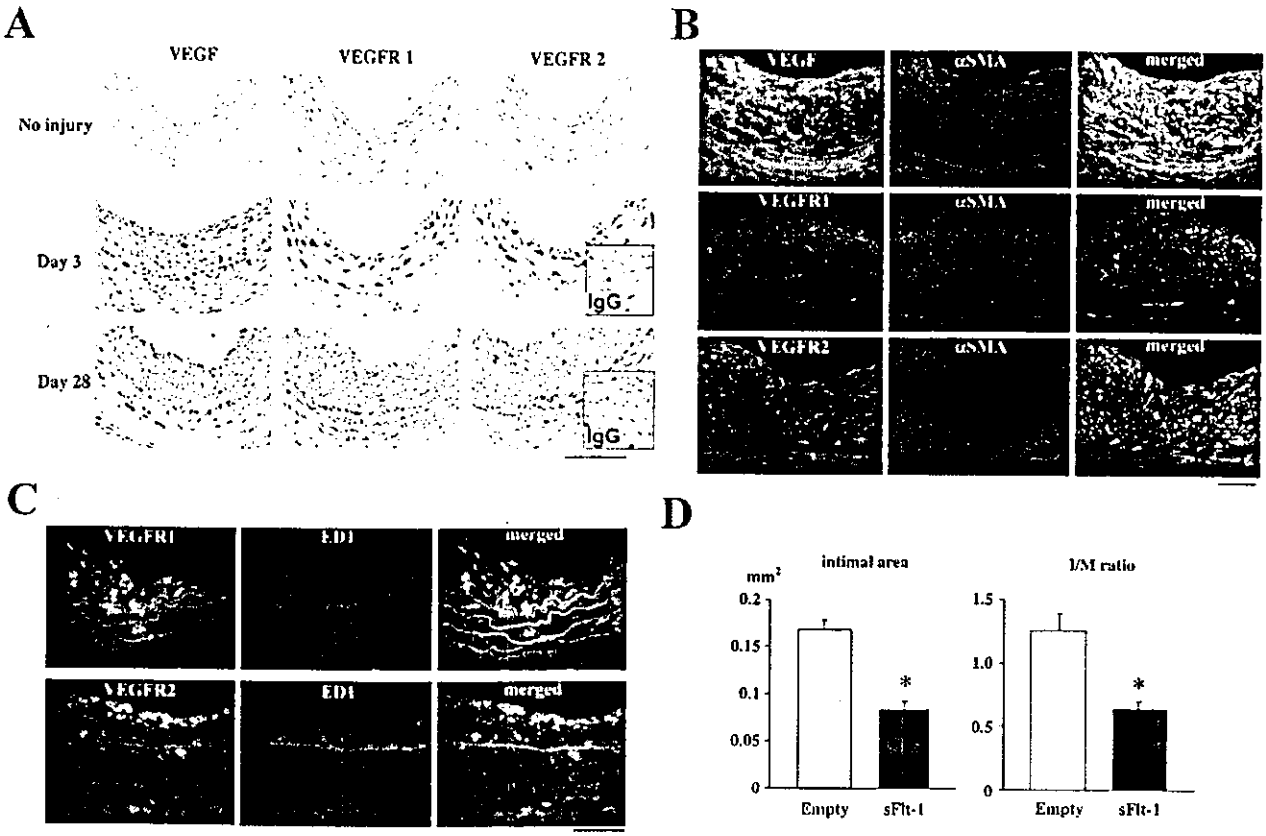

Figure 2. Expression of VEGF and its receptors after balloon injury and inhibitory effects of *sFlt-1* gene transfer on neointimal formation in rats. A, Immunohistochemistry of arterial cross-sections stained immunohistochemically with VEGF, VEGFR-1 (Flt-1), or VEGFR-2 (Flk-1). Bar indicates 100 μm. B, Fluorescence double immunohistochemistry 28 days after balloon injury. Photomicrographs show injured arteries stained with VEGF, VEGF-R1 (Flt-1), or VRGFR-2 (Flk-1) in green. Photomicrographs show injured arteries also stained with α-smooth muscle actin in red. Single-fluorescence–positive cells were stained in green or red, whereas double-positive cells were stained in yellow. Scale bar indicates 100 μm. C, Fluorescence double immunohistochemistry 7 days after balloon injury. Photomicrographs show injured arteries stained with VEGF-R1 or VEGF-R2 in green. Photomicrographs show injured arteries also stained with ED1 in red. Single-fluorescence–positive cells were stained in green or red, whereas double-positive cells were stained in yellow. Scale bar indicates 100 μm. D, Neointimal formation (neointimal area and intima-media ratio) on 28 day after balloon injury. *$P<0.01$ vs empty-plasmid group, n=8 or 9.

formation was also less in the *sFlt-1* group than in the empty-plasmid group on day 28 (Figure 2D).

To assess transfection efficacy of *sFlt-1*, plasma sFlt-1 concentration was measured in rabbits. The plasma sFlt-1 levels were 96±14, 377±25 ($P<0.01$ versus before), 413±20 ($P<0.01$), 284±15 ($P<0.05$), and 113±16 ($P>0.1$) pg/mL before and at 3, 7, 14, and 28 days after *sFlt-1* transfection, respectively, indicating that sFlt-1 was released from the transfected muscle to the circulation.

No Significant Effects of *sFlt-1* Gene Transfer on Endothelial Regeneration in Rabbits and Mice

In rabbits, there were no significant differences between the empty-plasmid and *sFlt-1*–transfected groups in the ratio of luminal surface area covered with endothelium (Figure 4A) and that of the CD31-positive endothelial layer 7 days after injury (Figure 4B). In mice, endothelial recovery was scarcely observed on day 7 (data not shown) but was noted equally in the 2 groups on day 14 (Figure 4C).

Inhibitory Effects of *sFlt-1* Transfer on Expression of Proinflammatory Factors

sFlt-1 transfection reduced the increased gene expression of MCP-1, platelet-derived growth factor, transforming growth factor-β, IL-1β, IL-6, tumor necrosis factor-α, matrix metalloproteinase-9, and VEGF (Figure 5A). *sFlt-1* transfer did not affect the increased gene expression of matrix metalloproteinase-1 and tissue factor. Immunohistochemical staining performed 7 days after balloon injury revealed increased immunoreactive MCP-1 and IL-1β in cells in the neointima and smooth muscle cells in the media, which were attenuated by *sFlt-1* gene transfer (Figure 5B).

Contribution of Bone Marrow Cells to the Effect of *sFlt-1* Gene Transfer in Mice

As reported,[26] a considerable proportion of neointimal and medial cells were LacZ-positive 28 days after injury in mice whose bone marrow expressed LacZ ubiquitously. Intimal area, intima-media ratio, and LacZ-positive cells were decreased in *sFlt-1*–transfected mice than in empty plasmid–

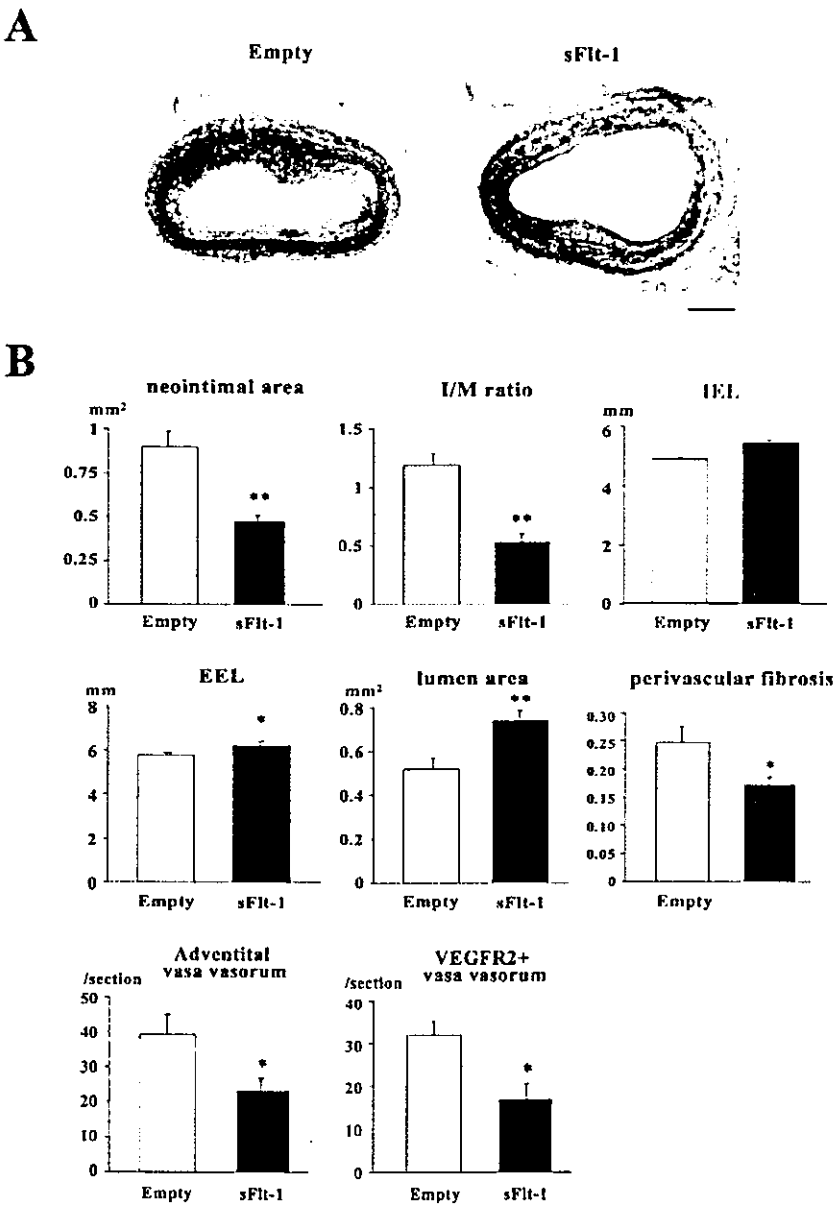

Figure 3. Inhibitory effect of *sFlt-1* gene transfer on restenotic changes (neointimal formation and negative remodeling) in rabbits. A, Carotid artery sections from empty-plasmid and *sFlt-1* groups 28 days after balloon injury stained with elastica van Gieson's stain. Bar=200 μm. B, Neointimal formation (neointimal area and intima-media ratio), negative remodeling (length of internal elastic lamina, length of external elastic lamina, and lumen area), perivascular fibrosis, adventitial vasa vasorum (number of CD31-positive vessels in adventitia), and VEGFR-2–positive vasa vasorum (number of VEGFR-2–positive vessels in adventitia) on day 28 after balloon injury are shown. $^{*}P<0.05$, $^{**}P<0.01$ vs empty-plasmid group, n=8 or 9.

transfected mice (Figure 6A and 6B). Wire injury also increased recruitment of bone marrow–derived monocytes (CD31-positive and c-Kit–positive) and circulating monocytes (Mac-1–positive) into peripheral blood (Figure 6C). *sFlt-1* gene transfer attenuated such changes in cell distribution, suggesting that wire injury increased such cell lineages in peripheral blood through VEGF. Plasma and femoral arterial concentrations of VEGF increased after wire injury, which was partly attenuated by *sFlt-1* transfection (online Tables III and IV).

Effects of $VEGF_{165}$ Gene Transfer on Neointimal Formation and Adventitial Angiogenesis in Rabbits

A recombinant adenoviral vector containing human $VEGF_{165}$ or the *LacZ* gene was produced. Gene transfer was performed by administering adenovirus solution (1 mL, 2×10^9 plaque-forming units) by a channel balloon catheter (Remedy, Boston Scientific Inc) immediately after balloon injury of rabbit carotid arteries (online Data Supplement and Figure). There were no significant differences between the empty-plasmid and *VEGF*-transfected groups in terms of neointimal formation, perivascular fibrosis, and negative remodeling (smaller lumen size, internal elastic lamina, and external elastic lamina) on day 28. In contrast, the number of adventitial vasa vasorum (the degrees of adventitial angiogenesis) was markedly increased in the *VEGF*-transfected group.

Discussion

VEGF has conventionally been thought to be an endothelial cell–specific growth factor and that it inhibits vascular pathological processes by accelerating endothelial proliferation and regeneration through endothelial VEGFR-2. If so, blockade of VEGF would suppress endothelial regeneration

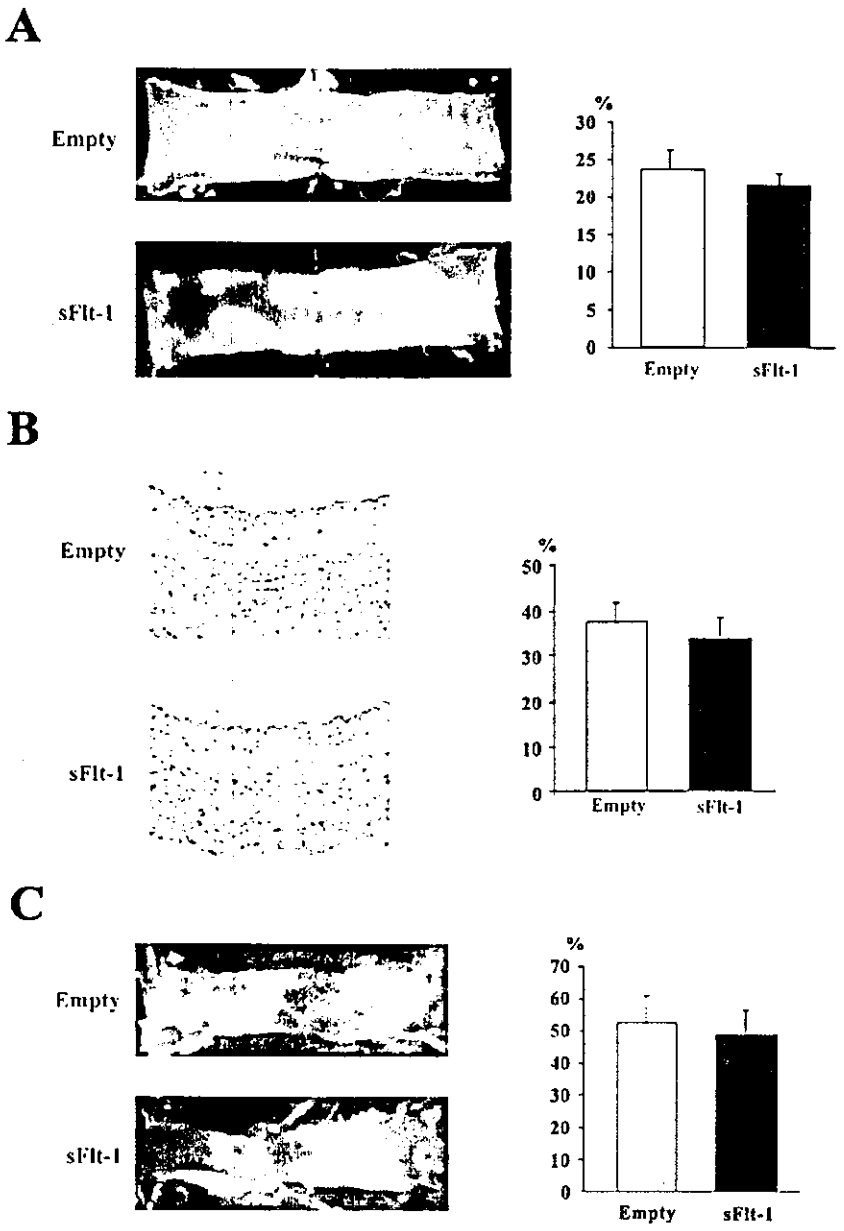

Figure 4. No significant effect of *sFlt-1* gene transfer on endothelial regeneration. A, Reendothelialization of rabbit carotid artery determined by Evans blue staining (deendothelialized areas are stained with blue) 7 days after balloon injury in rabbits. Endothelial regeneration of injured arteries was identified by intravenous injection of Evans blue dye 30 minutes before harvesting of vessels from rabbits and mice. Ratios of surface area covered by endothelium to total area in empty-plasmid and *sFlt-1* groups (n=7 each) are shown. B, Cross sections of rabbit femoral arteries stained with CD31 antibody 7 days after injury. Degrees of endothelial recovery (length of CD31-positive layer, length of internal elastic lamina in cross sections) in both groups are also shown (n=7 each). C, Reendothelialization of mouse femoral arteries 14 days after injury as determined by Evans blue staining (n=9 each).

and enhance neointimal formation after injury. In contrast to the conventional assumption, we here demonstrated that blockade of VEGF by *sFlt-1* gene transfer attenuated neointimal formation in rabbits, rats, and mice, indicating the essential role of VEGF in experimental restenosis.

As previously reported by others,[5-7,15] we demonstrated persistent increases in VEGF in arterial wall cells after injury. Emerging evidence suggests expression of functional VEGFR-1 and VEGFR-2 in cell types other than endothelial cells. We showed herein an increased expression of VEGFR-1 in lesional monocytes and medial smooth muscle cells during the early stage and in smooth muscle cells in the neointima and media during later stages. Increased VEGFR-2 expression was noted only at later stages. *sFlt-1* gene transfer attenuated the increased expression of inflammatory and growth factors such as VEGF, MCP-1, IL-1β, and so forth at early stages. Expression of VEGFR-1 in monocytes mediates chemotaxis,[9] and VEGFR-1 in smooth muscle cells mediates migration.[27] VEGFR-1 has been shown to act as an important mediator of VEGF-induced inflammation.[9,10,13] More recently, Yamada et al[28] showed that VEGF-mediated angiogenesis and inflammation are mediated by MCP-1. We also demonstrated the central role of MCP-1 in the mechanism of neointimal formation after vascular injury.[23-25,29] It is likely, therefore, that VEGF might cause vascular inflammation and migration of vascular smooth muscle cells and thus, cause neointimal formation after injury. Further studies are needed to elucidate the relative roles of VEGFR-1 and VEGFR-2 in the mechanisms of neointimal formation.

This study also demonstrated in rabbits the role of VEGF in the development of negative remodeling, another major cause of human restenosis after balloon angioplasty.[30] Fibro-

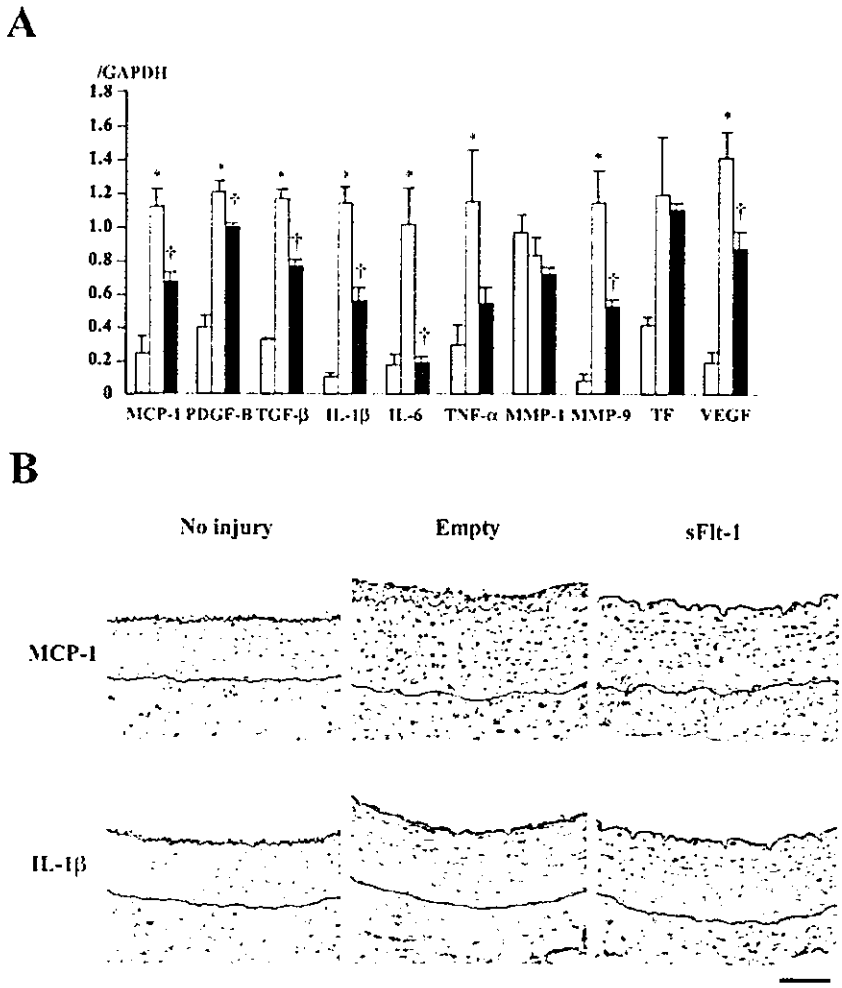

Figure 5. Inhibitory effect of *sFlt-1* gene transfer on expression of various inflammatory factors in rabbits. A, Effect of *sFlt-1* gene transfer on mRNA levels of various proinflammatory factors 1 day after injury. Quantitative real-time PCR was performed. *$P<0.01$ vs uninjured control (uninjured) artery; †$P<0.05$, ††$P<0.01$ vs empty-plasmid group. B, Carotid artery sections from control uninjured animals and those from empty-plasmid and *sFlt-1* groups 7 days after balloon injury stained immunohistochemically with MCP-1 and IL-1β. Internal and external elastic layers are highlighted with blue and black lines, respectively. Bar=100 μm. Immunohistochemical experiments were repeated 5 times, all with representative results.

sis and vasa vasorum in the adventitia have been implicated to be the central pathological processes leading to constrictive negative remodeling after balloon injury. Therefore, our present data suggest that *sFlt-1* gene transfer inhibited the development of negative constrictive remodeling by limiting adventitial fibrosis and angiogenesis.

VEGFR-1 has been shown to be an important mediator of stem cell recruitment and differentiation.[13] Sata and colleagues[26] have shown that a considerable proportion of neointimal and medial cells were bone marrow–derived progenitor cells. However, the role of VEGF in the recruitment and differentiation of progenitor cells into neointimal cells after vascular injury has not been addressed. We showed here that *sFlt-1* gene transfer inhibited recruitment of bone marrow–lineage cells into the peripheral circulation and injured arterial wall and thus, reduced neointimal formation after injury. These data suggest that VEGF might contribute to neointimal formation by recruiting bone marrow–derived and circulating monocytes.

Surprisingly, *sFlt-1* gene transfer did not affect endothelial regeneration after endothelial injury, suggesting a minor role of endogenous VEGF in endothelial regeneration after endothelial injury. It remains to be determined whether inhibition of VEGFR-2–mediated activity of endothelial regeneration by *sFlt-1* gene transfer might have been overshadowed by other stimuli (eg, basic fibroblast growth factor, angiopoietins, etc). On the contrary, adenovirus-mediated gene transfer of *VEGF* enhanced adventitial angiogenesis but did not reduce neointimal formation after balloon injury in rabbits. The latter observation is consistent with previous reports demonstrating that exogenous VEGF does not reduce neointimal formation in animals and humans.[15–17] Taken together, the role or mechanisms of action of VEGF may differ between exogenous and endogenous VEGF and between angiogenesis and neointimal formation.

This study may have significant clinical implications. First, *sFlt-1* gene transfer might be an attractive anti-VEGF therapy for inflammatory vascular disease and other inflammatory disorders. However, local delivery of *sFlt-1* must be preferable for clinical use to avoid potential side effects by systemic delivery. Second, our finding indicates that more research is required, especially on the safety of VEGF, before translational clinical research proceeds. Deleterious effects associated with overexpression of VEGF have recently been reported: (1) injection of VEGF-expressing skeletal muscle myoblasts into the murine heart caused the formation of hemangiomas and lethagenic heart failure[31] and (2) *VEGF* gene transfer into rabbit carotid arteries induced neointimal

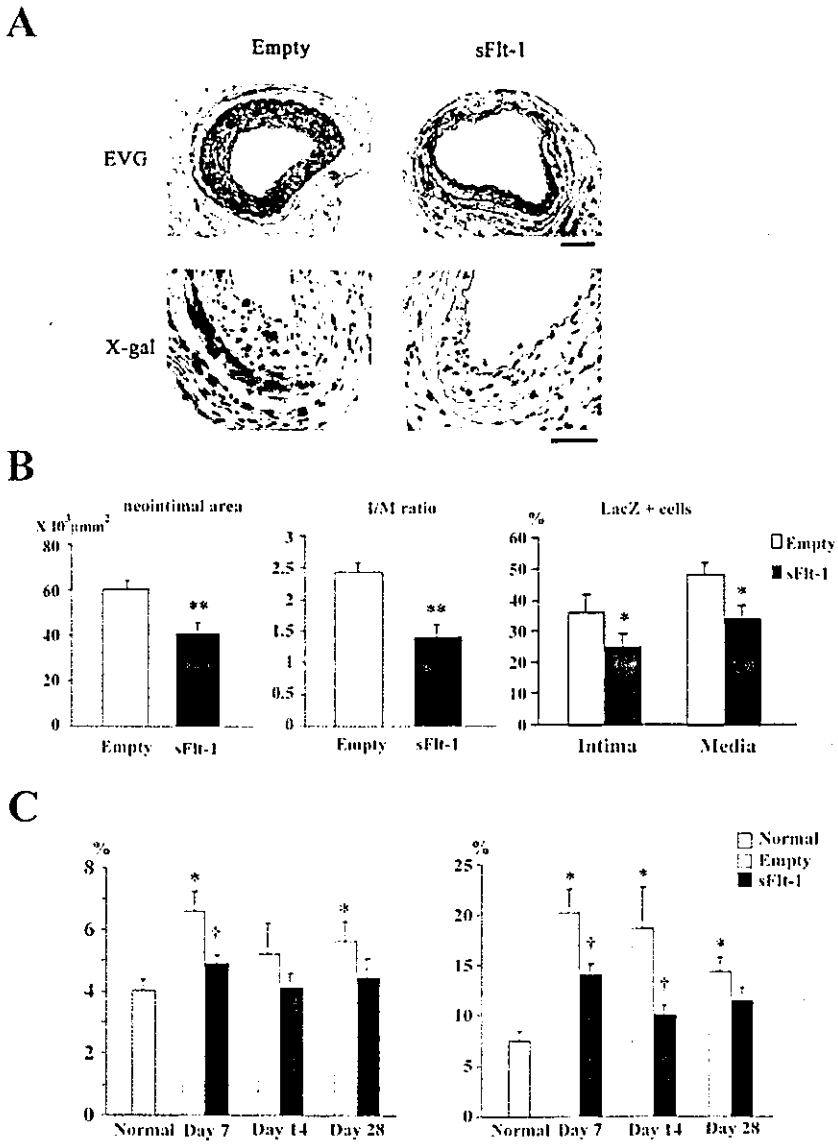

Figure 6. Contribution of bone marrow–derived cells to effect of *sFlt-1* gene transfer in mice. A, Arterial sections from empty-plasmid and *sFlt-1* groups 28 days after wire injury stained with X-gal or elastica van Gieson's (EVG) stains. Bar=100 μm. B, Inhibitory effects of *sFlt-1* gene transfer on neointimal formation (neointimal area and intima-media ratio) and percentage of LacZ-positive cells (100×LacZ-positive nuclei/total nuclei) in neointima and media. *$P<0.05$, **$P<0.01$ vs phosphate-buffered saline, n=8 each. C, Summary of fluorescence-activated cell sorting analysis of recruitment of bone marrow–derived monocytes (left) and circulating monocytes (right) into peripheral circulation in normal mice and mice transfected with empty plasmid or *sFlt-1* after wire injury, n=7 or 8. *$P<0.05$ vs normal mice (no injury); †$P<0.05$ vs empty-plasmid group.

formation with angiomatoid proliferation of endothelial cells.[12] These studies highlight the potential side effects or toxicity that would against the clinical use of VEGF for therapeutic angiogenesis and restenosis.

In conclusion, this study has provided direct in vivo evidence suggesting that increased expression and activity of VEGF are essential for the development of experimental restenosis after intraluminal injury by recruiting monocyte-lineage cells. Although there is no clinical evidence suggesting enhancement of atherosclerosis or neointimal formation by VEGF therapy,[16,17] our present data raise the question of whether VEGF therapy is useful without serious risks in patients with advanced atherosclerosis.

Acknowledgments

This study was supported by grants-in-aid for scientific research (14657172, 14207036) from the Ministry of Education, Science, and Culture, Tokyo, Japan; by health science research grants (Comprehensive Research on Aging and Health and Research on Translational Research) from the Ministry of Health Labor and Welfare, Tokyo, Japan; and by the Program for Promotion of Fundamental Studies in Health Sciences of the Organization for Pharmaceutical Safety and Research, Tokyo, Japan.

References

1. Folkman J. Angiogenesis in cancer, vascular, rheumatoid and other disease. *Nat Med.* 1995;1:27–31.
2. Carmeliet P, Jain RK. Angiogenesis in cancer and other diseases. *Nature.* 2000;407:249–257.
3. Ferrara N, Alitalo K. Clinical applications of angiogenic growth factors and their inhibitors. *Nat Med.* 1999;5:1359–1364.
4. Baumgartner I, Isner JM. Somatic gene therapy in the cardiovascular system. *Annu Rev Physiol.* 2001;63:427–450.
5. Inoue M, Itoh H, Ueda M, et al. Vascular endothelial growth factor (VEGF) expression in human coronary atherosclerotic lesions: possible pathophysiological significance of VEGF in progression of atherosclerosis. *Circulation.* 1998;98:2108–2116.
6. Chen YX, Nakashima Y, Tanaka K, et al. Immunohistochemical expression of vascular endothelial growth factor/vascular permeability factor in atherosclerotic intimas of human coronary arteries. *Arterioscler Thromb Vasc Biol.* 1999;19:131–139.
7. Shibata M, Suzuki H, Nakatani M, et al. The involvement of vascular endothelial growth factor and flt-1 in the process of neointimal prolif-

eration in pig coronary arteries following stent implantation. *Histochem Cell Biol.* 2001;116:471–481.
8. Isner JM. Still more debate over VEGF. *Nat Med.* 2001;7:639–640.
9. Barleon B, Sozzani S, Zhou D, et al. Migration of human monocytes in response to vascular endothelial growth factor (VEGF) is mediated via the VEGF receptor flt-1. *Blood.* 1996;87:3336–3343.
10. Kim I, Moon SO, Hoon Kim S, et al. Vascular endothelial growth factor expression of intercellular adhesion molecule-1 (ICAM-1), vascular cell adhesion molecule-1 (VCAM-1), and E-selectin through nuclear factor-κB activation in endothelial cells. *J Biol Chem.* 2001;276: 7614–7620.
11. Marumo T, Schini-Kerth VB, Busse R. Vascular endothelial growth factor activates nuclear factor-κB and induces monocyte chemoattractant protein-1 in bovine retinal endothelial cells. *Diabetes.* 1999;48: 1131–1137.
12. Yonemitsu Y, Kaneda Y, Morishita R, et al. Characterization of in vivo gene transfer into the arterial wall mediated by the Sendai virus (hemagglutinating virus of Japan) liposomes: an effective tool for the in vivo study of arterial diseases. *Lab Invest.* 1996;75:313–323.
13. Luttun A, Tjwa M, Moons L, et al. Revascularization of ischemic tissues by PlGF treatment, and inhibition of tumor angiogenesis, arthritis and atherosclerosis by anti-Flt1. *Nat Med.* 2002;8:831–40.
14. Celletti FL, Waugh JM, Amabile PG, et al. Vascular endothelial growth factor enhances atherosclerotic plaque progression. *Nat Med.* 2001;7: 425–429.
15. Hiltunen MO, Laitinen M, Turunen MP, et al. Intravascular adenovirus-mediated VEGF-C gene transfer reduces neointima formation in balloon-denuded rabbit aorta. *Circulation.* 2000;102:2262–2268.
16. Hedman M, Hartikainen J, Syvanne M, et al. Safety and feasibility of catheter-based local intracoronary vascular endothelial growth factor gene transfer in the prevention of postangioplasty and in-stent restenosis and in the treatment of chronic myocardial ischemia: phase II results of the Kuopio Angiogenesis Trial (KAT). *Circulation.* 2003;107: 2677–2683.
17. Henry TD, Annex BH, McKendall GR, et al. The VIVA trial: Vascular endothelial growth factor in Ischemia for Vascular Angiogenesis. *Circulation.* 2003;107:1359–1365.
18. Kendall RL, Wang G, Thomas KA. Identification of a natural soluble form of the vascular endothelial growth factor receptor, FLT-1, and its heterodimerization with KDR. *Biochem Biophys Res Commun.* 1996;226: 324–328.
19. Zhao Q, Egashira K, Inoue S, et al. Vascular endothelial growth factor is necessary in the development of arteriosclerosis by recruiting/activating monocytes in a rat model of long-term inhibition of nitric oxide synthesis. *Circulation.* 2002;105:1110–1115.
20. Goldman CK, Kendall RL, Cabrera G, et al. Paracrine expression of a native soluble vascular endothelial growth factor receptor inhibits tumor growth, metastasis, and mortality rate. *Proc Natl Acad Sci U S A.* 1998; 95:8795–8800.
21. Losordo DW, Vale PR, Hendel RC, et al. Phase 1/2 placebo-controlled, double-blind, dose-escalating trial of myocardial vascular endothelial growth factor 2 gene transfer by catheter delivery in patients with chronic myocardial ischemia. *Circulation.* 2002;105:2012–2018.
22. Kondo K, Hiratsuka S, Subbalakshmi E, et al. Genomic organization of the flt-1 gene encoding for vascular endothelial growth factor (VEGF) receptor-1 suggests an intimate evolutionary relationship between the 7-Ig and the 5-Ig tyrosine kinase receptors. *Gene.* 1998;208:297–305.
23. Usui M, Egashira K, Ohtani K, et al. Anti-monocyte chemoattractant protein-1 gene therapy inhibits restenotic changes (neointimal hyperplasia) after balloon injury in rats and monkeys. *FASEB J.* 2002;16: 1838–1840.
24. Mori E, Komori K, Yamaoka T, et al. Essential role of monocyte chemoattractant protein-1 in development of restenotic changes (neointimal hyperplasia and constrictive remodeling) after balloon angioplasty in hypercholesterolemic rabbits. *Circulation.* 2002;105:2905–2910.
25. Egashira K, Zhao Q, Kataoka C, et al. Importance of monocyte chemoattractant protein-1 pathway in neointimal hyperplasia after periarterial injury in mice and monkeys. *Circ Res.* 2002;90:1167–1172.
26. Sata M, Saiura A, Kunisato A, et al. Hematopoietic stem cells differentiate into vascular cells that participate in the pathogenesis of atherosclerosis. *Nat Med.* 2002;8:403–409.
27. Wang H, Keiser JA. Vascular endothelial growth factor upregulates the expression of matrix metalloproteinases in vascular smooth muscle cells: role of flt-1. *Circ Res.* 1998;83:832–840.
28. Yamada M, Kim S, Egashira K, et al. Molecular mechanism and role of endothelial monocyte chemoattractant protein-1 induction by vascular endothelial growth factor. *Arterioscler Thromb Vasc Biol.* 2003;23: 1996–2001.
29. Egashira K. Molecular mechanisms mediating inflammation in vascular disease: special reference to monocyte chemoattractant protein-1. *Hypertension.* 2003;41:834–841.
30. Kakuta T, Currier JW, Haudenschild CC, et al. Differences in compensatory vessel enlargement, not intimal formation, account for restenosis after angioplasty in the hypercholesterolemic rabbit model. *Circulation.* 1994;89:2809–2815.
31. Lee RJ, Springer ML, Blanco-Bose WE, et al. VEGF gene delivery to myocardium: deleterious effects of unregulated expression. *Circulation.* 2000;102:898–901.

Diagnostic Value of the Recovery Time-Course of ST Slope on Exercise ECG in Discriminating False- From True-Positive ST-Segment Depressions

Satoru Sakuragi, MD; Hiroshi Takaki, MD; Atsushi Taguchi, MD; Kazuhiro Suyama, MD; Takashi Kurita, MD; Wataru Shimizu, MD; Toru Kawada, MD; Yoshio Ishida, MD; Tohru Ohe, MD; Kenji Sunagawa, MD

Circulation Journal
Vol. 68 No. 10 October 2004
(Pages 915–922)

Circ J 2004; **68**: 915–922

Diagnostic Value of the Recovery Time-Course of ST Slope on Exercise ECG in Discriminating False- From True-Positive ST-Segment Depressions

Satoru Sakuragi, MD; Hiroshi Takaki, MD*; Atsushi Taguchi, MD; Kazuhiro Suyama, MD; Takashi Kurita, MD; Wataru Shimizu, MD; Toru Kawada, MD*; Yoshio Ishida, MD**; Tohru Ohe, MD†; Kenji Sunagawa, MD*

Background Using the exercise ECG for diagnosing coronary artery disease (CAD) is hampered by the occurrence of false-positive (FP) ST-segment depression. Because it is known that the recovery ST-T time-course in CAD differs from that in FP subjects, the ST slope may help discriminate FP from true-positive (TP) results.
Methods and Results Treadmill digitized ECG from patients with significant ST-segment depressions and normal resting ECG were analyzed in 134 patients with CAD on angiography (>50% narrowing) and reversible perfusion defects (TP group), and 64 subjects with normal perfusion (FP group) on exercise single photon emission computed tomography. The ST slope between the J-point and J80 was measured every minute up to 6-min postexercise. The ST slope was significantly higher in FP than in TP at peak exercise, and at postexercise 1-, 2- and 3-min ($p<0.01$, all). Thereafter, it gradually increased in TP, while monotonically decreasing in FP. Its decrease from 3- to 6-min could correctly diagnose 88% of FP subjects, whereas it was found in only 19% of TP patients (total accuracy 83%).
Conclusions The ST slope change from early to late recovery is a simple yet reliable marker for discriminating FP from TP ST-segment responses in subjects with a normal resting ECG. (*Circ J* 2004; **68**: 915–922)

Key Words: Coronary disease; Electrocardiography; Exercise; Ischemia

Gender and several anatomical and functional characteristics are associated with an increased incidence of abnormal ST-segment responses to exercise in the absence of coronary artery disease (CAD). Subsets with an increased incidence of false-positive (FP) exercise ECG responses with respect to ischemia include middle-aged women[1-3] and patients with mitral valve prolapse[1,4,5] Patients with left ventricular hypertrophy (LVH) form a separate subset with the potential for inadequate myocardial perfusion in the absence of significant CAD[4,6] Advanced ECG analysis approaches applicable to the clinical evaluation of the standard exercise ECG in these subjects are currently unavailable and need to be developed.

The ST slope, usually computed as the slope between the J-point and the J80, has been mainly used for differentiating the configuration of ST-segment depression (ie, upsloping, horizontal, and downsloping). The latter two are considered more specific for myocardial ischemia than the upsloping shape[1,7] However, in CAD, the shape often changes with time during the test and a relatively characteristic time-course can be seen. ST-segment depression during exercise changes from upsloping (or horizontal) to downsloping in the early recovery at 2–4 min; that is, the ST slope decreases in early recovery (Fig 1A)[7,8] Subsequently, both ST-segment depression and the ST slope return gradually toward the baseline; that is, the ST slope increases in late recovery. On the other hand, in many subjects with FP ST-segment depression (FPD) (Fig 1B), the downsloping shape appears, not in the early, but in the late recovery. Unlike in CAD, the ST slope monotonically decreases from early to late recovery, possibly serving as the differentiating characteristic[5,8]

We thus hypothesized that the temporal changes in the ST slope from early to late recovery are capable of differentiating these 2 groups and we performed high-resolution computer analysis of the ST slope in the recovery in a relatively large population with normal resting ECGs. Because the majority of subjects with normal exercise single-photon emission computed tomography (SPECT) results are no longer referred for coronary angiography in the clinical practice, we used this technique for the selection of FPD subjects. True-positive (TP) results were defined when both angiographic and exercise SPECT images were abnormal.

Methods

Study Population

From the digitized ECG recordings consecutively obtained during routine treadmill testing for the evaluation of CAD, 198 patients (62±9 years) with an exercise-induced significant ST-segment depression were recruited. Patients were excluded if they had resting ECG abnor-

(Received February 3, 2004; revised manuscript received July 7, 2004; accepted July 13, 2004)
*Division of Cardiology, Department of Medicine, National Cardiovascular Center, *Department of Cardiovascular Dynamics, National Cardiovascular Center Research Institute, **Department of Radiology and Nuclear Medicine, National Cardiovascular Center, Suita and †Department of Cardiovascular Medicine, Okayama University Graduate School of Medical and Dentistry, Okayama, Japan*
Mailing address: Hiroshi Takaki, MD, Department of Cardiovascular Dynamics, National Cardiovascular Center Research Institute, 5-7-1 Fujishiro-dai, Suita 565-8565, Japan. E-mail: htakaki@res.ncvc.go.jp